



Research papers



Modeling the evolution of water-environment-economy coupling system with the impacts of inter-basin water transfer project

Danni Jia ^a, Jingwen Zhang ^{a,*}, Zejun Li ^b, Maoyuan Feng ^c, Kairong Lin ^a, Xiaohong Chen ^a, Xiaohui Lei ^d, Lixin He ^d, Chao Ma ^e, Jingru Ji ^a

^a Center for Water Resources and Environment, Guangdong Key Laboratory of Marine Civil Engineering, School of Civil Engineering, Sun Yat-sen University, Guangzhou 510275, China

^b Guangdong Research Institute of Water Resources and Hydropower, Guangzhou, China

^c Biogeochemistry and Modelling of the Earth System-BGEOSYS, Department of Geoscience, Environment and Society, Université Libre de Bruxelles, Brussels, Belgium

^d School of Water Resources and Electric Power, Hebei University of Engineering, 056038 Handan, China

^e State Key Laboratory of Hydraulic Engineering Simulation and Safety, Tianjin University, Tianjin 300072, China

ARTICLE INFO

This manuscript was handled by Amilcare Porporato, Editor-in-Chief, with the assistance of Rachata Muneepeerakul, Associate Editor

Keywords:

Inter-basin water transfer
Water-environment-economy system
System dynamics model
South-to-north water transfer middle route project
Climate change

ABSTRACT

Inter-Basin Water Transfer (IBWT) projects are playing an increasingly critical role in alleviating regional water scarcity and ensuring national water security goals. However, the impacts of IBWT projects on the complex interactions of the Water-Environment-Economy (WEE) system in water-receiving areas have seldom been addressed. This study develops a system dynamics (SD) model to capture the complex feedback loops governing the WEE system in water-receiving areas. Six nonlinear ordinary differential equations are constructed to represent the dynamics of population, GDP, CO₂ emissions, crop area, environmental awareness, and water demand. These equations are driven by key exogenous variables, including water transfer capacity, temperature, and precipitation. Taking Hebei province, one of the major water-receiving areas of the South-to-North Water Transfer Middle Route Project (MRP) of China, as a case study, the proposed model demonstrates strong capability in simulating the historical evolution trajectories of the WEE system. Results indicate that the evolution of the WEE system is characterized by cyclical patterns of total water demand, progressing through four phases: expansion (stage 1 from 2002 to 2015), degradation (stage 2 from 2016 to 2048), recovery (stage 3 from 2049 to 2084), and stability (stage 4 from 2085 to 2100). Water demand in the receiving areas is projected to peak around 2085 under the SSP245 scenario, while carbon emissions have already peaked in 2016. The sensitivity analysis of model parameters has demonstrated the robustness of the proposed SD model for the WEE system in Hebei regions. The external factors, including climate change and water transfer capacity of MRP, have pronounced impacts on the evolutionary trajectory of the WEE system. Enhancing the water transfer capacity of the IBWT project under this scenario contributes to the economy development. This research provides deeper insights into WEE system dynamics with the impacts of IBWT, offering a scientific basis for enhanced water resource management and sustainable development strategies in water-receiving areas.

1. Introduction

Water shortage is still a severe problem across the globe that constrains the regional socio-economic development and leads to ecological and environmental degradation (Dong et al., 2023; Sun et al., 2018). In the last century, human activities are increasingly intensive, reflected by the population growth, industrial expansion, and agricultural intensification (Zabel et al., 2019). Thus, the water demand is projected to increase by 50–80 % over the next 30 years (Flörke et al., 2018; Garrick

et al., 2019). The competition between different water use sectors for limited water resources will exacerbate water scarcity. As a result, the water scarcity can negatively impact both economic production and the environment, which will in return intensify the competition and accelerate the water scarcity, forming a feedback loop in the Water-Economy-Environment (WEE) system. Finally, this feedback loop will create significant challenges for achieving the Sustainable Development Goals (Larsen et al., 2016; United Nations (UN) (2015)). Water is essential for sustaining economic growth and maintaining ecological balance in the

* Corresponding author.

E-mail address: zhangjw269@mail.sysu.edu.cn (J. Zhang).

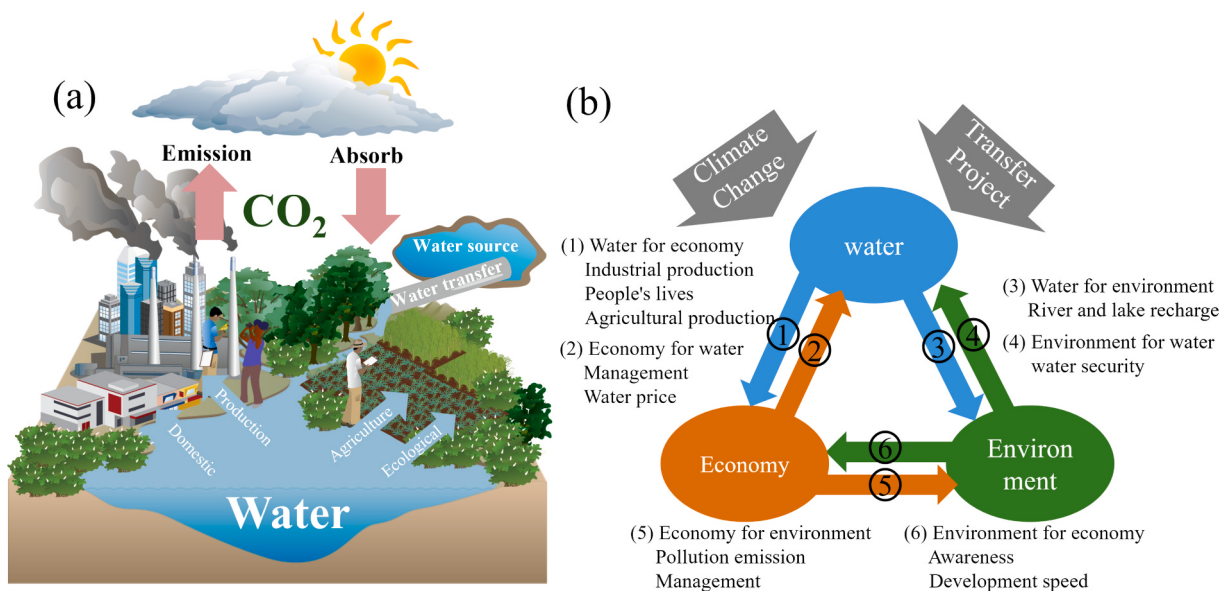


Fig. 1. Conceptualization of a general WEE coupling system. (a) A generalized map of natural processes and human activities involved in the water-receiving areas of a IBWT project. (b) The interconnections across water, economy, and environment subsystems.

WEE system, particularly in rapidly developing regions (Du et al., 2023; Sun et al., 2018; Zeng et al., 2022). A human–nature coupled WEE system is essential for addressing these stresses and has become a key factor in achieving sustainable development.

The Inter-Basin Water Transfer (IBWT) projects have become essential strategies to alleviate water scarcity, while also addressing constraints on regional economic or environmental development. Up to year 2015, more than 160 major inter-basin water transfer projects have been implemented across 20 countries (Dobbs et al., 2023; Faúndez et al., 2023), such as the South-to-North Water Transfer Project in China, the California Water Project in the United States, and the Canadian water transfer projects (Brown Jr., 1968; Niu, 2022; Siddik et al., 2023). In particular, China has advanced a batch of major projects that forms the national water network to solve or at least alleviate the water shortage problems across China (Government of the People's Republic of China, 2023), and IBWT is considered as the backbone of the national water network. IBWT projects have effectively alleviated water scarcity in water-receiving areas, supporting economic growth and environmental sustainability. Given the growing importance of IBWT projects, there is an urgent need to investigate their impacts on the WEE coupling systems. In recent years, many studies have investigated the complex interactions among WEE systems. For example, Wang et al. (2025) developed a multi-scale modeling framework integrating hydrological simulation with feedback loop analysis to examine the water-hydropower-environment nexus in the Hanjiang River Basin. Zhao et al. (2023) proposed a sensitivity-based framework that incorporates community sensitivity to identify key feedbacks and analyze the coevolution of the water-energy-environment nexus under different urbanization patterns in the Wuhan. Zhu et al. (2025) developed a dynamic co-optimization model integrating multiple factors and regulatory mechanisms to enhance the synergy of the water-agriculture-ecology system in the Shiyang River Basin. Zhao et al. (2023) proposed a sensitivity-based framework that incorporates community sensitivity to identify key feedbacks and analyze the coevolution of the water-energy-environment nexus under different urbanization patterns in the Wuhan. Zhu et al. (2025) developed a dynamic co-optimization model integrating multiple factors and regulatory mechanisms to enhance the synergy of the water-agriculture-ecology system in the Shiyang River Basin. However, these studies mainly focused on the water subsystem with local water supply, without the impacts of the transferred water from the IBWT projects. This

limitation hinders the simulation of the evolution of WEE system in water-receiving areas and the identification of potential emergent phenomena that may arise during the operation of IBWT projects. Moreover, the impacts of water transfers on the economy and environment in water-receiving areas remains difficult to be quantified, making it challenging to predict their long-term effects and regional evolutionary trends comprehensively.

Various system analysis techniques have been developed to model complex coupled systems, aiming to understand the co-evolution of humans and water resources systems (Di Baldassarre et al., 2013; Zhao et al., 2023). These techniques include system dynamics (SD) models (Amirkhani et al., 2022; He et al., 2025; Zhou et al., 2025), system of systems models (Housh et al., 2015; Tan et al., 2021), complex network analysis, and agent-based models (Chen et al., 2016; Ng et al., 2011; Wang et al., 2018; Wang et al., 2023). System of systems models can coordinate interactions among multiple interdependent subsystems. Complex network analysis helps identify critical nodes and relationships in nexus systems, while agent-based models are useful for simulating stakeholders' decision-making behaviors in socio-ecological systems. While various modeling approaches are capable of representing feedback to some extent, they often lack a systemic treatment of dynamic and nonlinear feedbacks within coupled systems, where SD models demonstrate particular strengths (Abolghasemzadeh et al., 2024; Coletta et al., 2024; Richardson, 2020). SD is a methodology for modeling and analyzing the behavior of complex systems over time, particularly in scenarios involving feedback loops and time delays. Primarily driven by exogenous variables, SD aims to uncover the endogenous structures underlying typically complex and intricate dynamics of natural-human coupled systems (Forrester, 1968). Moreover, it is capable of handling complex nonlinear and temporal relationships among variables. This capability makes it particularly suitable for exploring the co-evolution of WEE coupling system in water-receiving areas of IBWT projects. Therefore, employing SD to conduct comprehensive research in water-receiving areas of IBWT projects is essential for accurately predicting long-term system evolution and informing adaptive management strategies.

The primary goal of this study is to explore the evolutionary trajectories of the WEE coupling systems in the water-receiving areas of the IBWT projects under climate change. This is achieved through three main aspects: (1) establishing a comprehensive analytical framework of the WEE coupling system in water-receiving areas of the IBWT project,

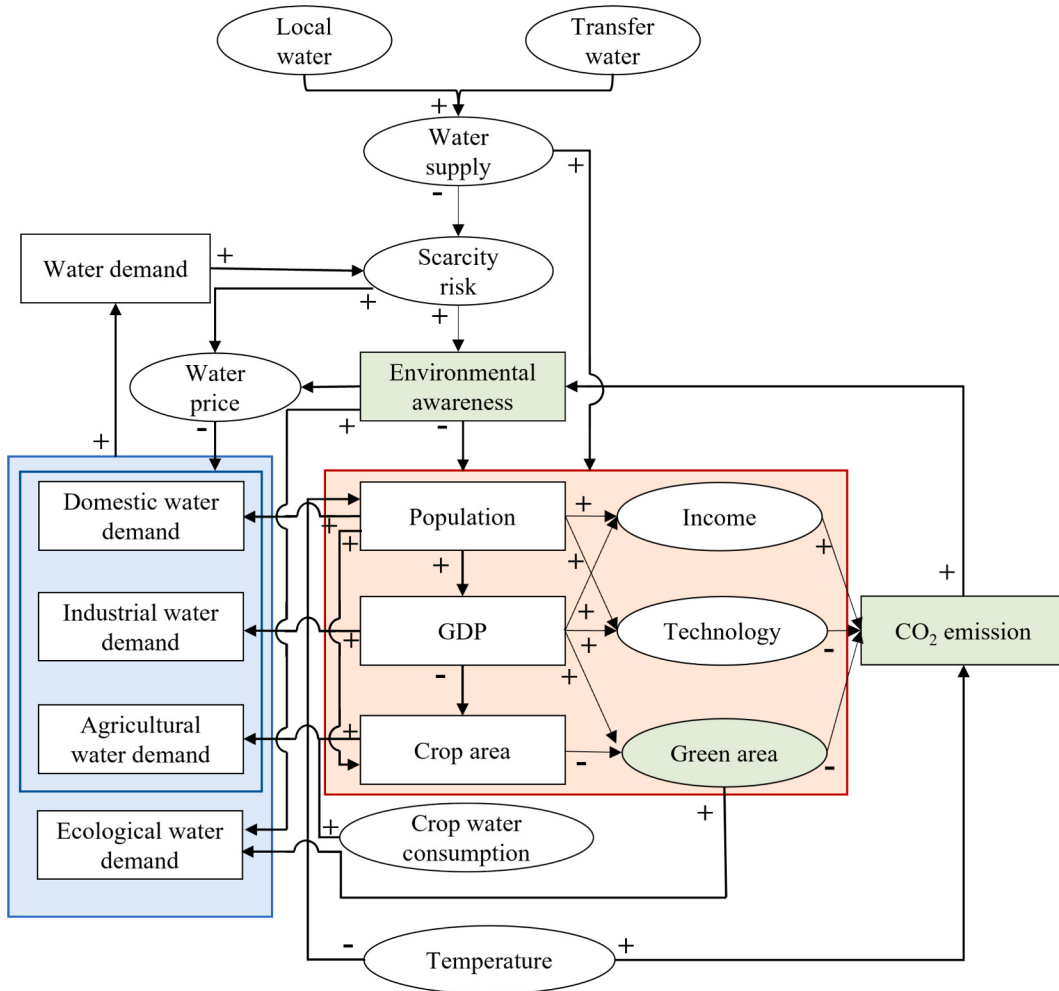


Fig. 2. Sketch of complex interconnections of WEE coupling system. Red background represents the economy subsystem, blue represents the water resources subsystem, and green represents the environment subsystem. Rectangles represent governing variables, and ovals represent auxiliary and driving variables. (For interpretation of the references to colour in this figure legend, the reader is referred to the web version of this article.)

which highlights the complex feedback mechanisms among the water resources, the environment, and the economy subsystems; and (2) incorporating carbon emissions and latent variables (environmental awareness and technological progress), to better capture socio-economic and environmental feedbacks; (3) exploring the evolutionary trajectories of the WEE coupling system under multiple scenarios, including different water transfer capacities of the IBWT project and projected future climate change conditions. The proposed framework provides a robust foundation for understanding the dynamic responses of WEE coupling systems to both IBWT projects and external drivers, thereby supporting informed decision-making for sustainable regional development.

2. Methodology

The system dynamics (SD) modeling framework is developed based on a set of lumped nonlinear differential equations to capture the key interactions within the WEE coupling system. The fundamental principles of WEE interactions, including coupling mechanisms and internal feedback loops, are introduced in Section 2.1. The evolution of state variables is described by nonlinear ordinary differential equations, which serve as the governing equations of the system (Section 2.2). Socio-economic interactions and external driving forces are incorporated through constitutive relationships statistically derived from empirical datasets, as explained in Section 2.3. Sensitivity analysis is

conducted to identify the most influential parameters affecting system behavior (Section 2.4). Finally, scenario-based simulations are implemented using the established model to explore system responses under varying climate conditions and policy scenarios, as presented in Section 2.5.

2.1. Model conceptualization

The SD model of the WEE coupling system is mainly divided into three subsystems, including water resources, environment, and economy subsystems, impacted by the external factors, such as climate change and the amount of transferred water (Fig. 1). Among these, the water subsystem is central to the SD model, playing a pivotal role in shaping the interactions and feedbacks within the WEE coupling system. Water availability is fundamental to supporting urban domestic, industrial, and agricultural development, and is particularly critical for maintaining environmental sustainability. In addition, water availability critically constrains on the WEE system's synergy and determines its development trajectory through threshold effects in IBWT's water-receiving areas. The economy subsystem, as the human-driven component of the WEE system, is highly dynamic and adaptive. It directly influences water and environment subsystems through industrial production, agricultural irrigation, and other socio-economic activities that involve water consumption and lead to CO₂ emissions. Rapid economic growth exacerbates the severity of water scarcity, while

simultaneously fostering heightened environmental awareness and triggering self-regulatory feedback mechanisms that curb unsustainable development.

The environment subsystem is significantly impacted by human activities, such as fossil fuel combustion, industrial production, deforestation, and intensive agricultural practices (Chen and Chen, 2016). These activities have led to a sustained increase in CO₂ emissions, affecting climate change and thus disrupting the natural water cycle. In this context, reducing carbon emissions become particularly important in the environment subsystem. The external factors primarily represent the climate change (i.e. temperature) and the water transferred capacities. Specifically, changes in temperature can alter both precipitation patterns and evapotranspiration rates, thereby affecting the availability of local water resources. Meanwhile, the IBWT project supplements water supply to receiving areas, enhancing circulation and interaction within the WEE coupling system.

Based on the above conceptualization, several important variables can be identified to represent the governing variables of different subsystems. The economy subsystem primarily includes variables such as population (P), GDP, and agricultural crop area (A). Population and GDP are used to characterize the economic scale and growth rate of the water-receiving areas of the IBWT project, while crop area primarily reflects the regional agricultural water demand. The environment subsystem includes CO₂ emissions (CO₂), green area (A_g), and environmental awareness (E). Environmental awareness reflects the level of societal attention to environment and water resource subsystems during current development. Green area serves as an indirect metric to quantify ecological water demand. The water resources subsystem comprises water demand (DW), water price (P_r), and water scarcity risk (S). Water demand, as a primary governing variable of the water subsystem, reflects the dynamic changes in water requirements in the water-receiving areas of IBWT project. It serves as a critical indicator in analyzing the interactions between water and other subsystems. Water price and scarcity risk act as auxiliary variables that influence water demand, indirectly adjusted by economic and environmental feedback mechanisms under prevailing conditions.

The complex relationships among system variables are illustrated in Fig. 2. Each interdependency generates feedback loops that affect overall system behavior, which is primarily driven by water resources and climate conditions. Environmental awareness serves as a key socio-behavioral factor that helps mediate the trade-offs between economic development and sustainable water resource management, especially under water scarcity. Population growth increases domestic water demand and concurrently promotes rapid GDP development, thereby driving greater industrial water consumption. Moreover, to meet the rising food demand, cropland expansion becomes necessary, which in turn further intensifies agricultural water use. Conversely, higher income levels can stimulate investments in water-saving technologies, reducing reliance on fossil fuels, and promote energy conservation and emission reduction, thus forming a positive feedback loop. Rising water demand may further exacerbate water scarcity, leading to increased environmental awareness. Consequently, this elevated environmental awareness may then suppress socio-economic growth, forming a negative feedback loop. Similar feedback loops can be identified throughout the complex WEE coupling system, revealing the intricate and interdependent nature of the system's internal dynamics.

2.2. Governing equations

The SD model for the WEE coupling system is primarily represented by differential equations for six governing variables and nonlinear functional relationships for six auxiliary variables. Population dynamics are represented using the logistic growth equation, which captures fundamental demographic trends. Economic development is modeled through the classical Cobb-Douglas production function, embedded within the GDP formulation. The equations for crop area and CO₂

emissions incorporate multiple driving factors, including economic, technology, climate, and water resources. Environmental awareness is described by an equation that reflects regional shifts in public attitudes towards water resource management and carbon emissions. Finally, water demand is predicted through a comprehensive framework that accounts for domestic, industrial, ecological, and agricultural water requirements, enabling a holistic assessment of total water requirements.

2.2.1. Population equation

The population equation is represented by the Logistic growth model (Tsoularis & Wallace, 2002), which captures population growth under limited resources (e.g., water, land, energy and etc.). This formulation aligns with demographic transition theory and is widely used in system modeling studies to project population growth under environmental and socio-economic constraints (Kumar & Lal, 2017; Zhang et al., 2025).

The growth rate ($r, \%$) and carrying capacity ($K, 1 \times 10^4$ people) are driven by temperature ($T, ^\circ\text{C}$), domestic water use ($W_d, 1 \times 10^8 \text{ m}^3$), and environmental awareness (E), capturing the coupled effects of climate, water availability, and societal responses on population trends. Rising temperature can threaten food security and intensify migration pressures, thereby reducing population growth and regional sustainability (Almulhim et al., 2024; Awad et al., 2024). Increased domestic water use improves living conditions and supports urban development, expanding the effective carrying capacity (He et al., 2021). Higher environmental awareness imposes stronger sustainability constraints, mitigating overpopulation pressure and promoting balanced development (Henson, 1994). The specific form is:

$$\frac{dP}{dt} = rP(1 - \frac{P}{K}) \quad (1)$$

$$r = r_0 + \alpha_1 T + \alpha_2 W_d \quad (2)$$

$$K = K_0 + \beta_1 W_d + \beta_2 E + \beta_3 T \quad (3)$$

where P represents the population (1×10^4 people), K_0 is the initial carrying capacity (1×10^4 people), α and β are the weighting coefficients representing the influence of different factors on the growth rate and carrying capacity, respectively.

2.2.2. Economic equation

The economic equation is determined based on the Cobb-Douglas (C-D) (Cobb & Douglas, 1928) production function, which characterizes the dynamic process of economic growth by attributing output changes to technological progress, capital, and labor through constant elasticities. This classical model has been widely applied in macroeconomic analyses and remains a fundamental tool for explaining the sources of economic growth (Basegmez & Onalan, 2018; Colther & Doussoulin, 2024).

Building on the classical form and considering the WEE interactions in water-receiving areas, we redefine the input variables to better reflect regional characteristics. Population (P) serves as a proxy for effective labor and demand, while industrial water use ($W_i, 1 \times 10^8 \text{ m}^3$) represents capital input, as water resources constitute a key production constraint in these regions. In addition, the initial technological development rate (TE_0) and environmental awareness (E) are incorporated to capture the combined effects of technological advancement and environmental regulation on economic growth. The specific form is:

$$\frac{dGDP}{dt} = TE_0 \times f(P)^\alpha \times f(W_i)^\beta \times f(E)^\varepsilon \quad (4)$$

where $\alpha, \beta, \varepsilon$ are the elasticity coefficients of population, water supply, and environmental, respectively.

2.2.3. CO₂ emission equation

Due to the complexity of the quantification of CO₂ emissions, a

response function approach is employed to represent the dynamic changes of CO₂ emissions (Chen et al., 2016; Van Emmerik et al., 2014; Zhao et al., 2023). This approach eliminates the need for direct measurements while indicating the relative magnitude and direction of improvement or deterioration. Conventional carbon emission accounting quantifies emissions from energy consumption in the agricultural, industrial, and residential sectors using energy conversion and emission factors, while excluding the carbon sequestration from ecosystems. In this framework, temperature (T) represents the climatic stress that exacerbates energy demand for heating and cooling (Wigley & Jones, 1981); green area (A_g , 104 ha) reflects human-driven environmental restoration and improvement efforts that contribute to emission reduction (Li et al., 2010); Technological level (TE) captures progress stimulated by economic growth due to improving energy efficiency and reducing emissions; and per capita disposable income (I , RMB) reflects the influence of economic affluence on consumption-related emissions (Mardani et al., 2019). These variables collectively describe the environmental, technological, and socioeconomic drivers of regional CO₂ emissions in water-receiving areas. The simplified CO₂ emission change rate can be expressed, such as:

$$\frac{dC}{dt} = f(T) - f(A_g) - f(TE) + f(I) \quad (5)$$

where CO₂ is the CO₂ emissions (1×10^8 tones).

2.2.4. Crop area equation

The changes of crop area are also quantified using a response function approach. Agricultural water supply, technological development, population, and GDP are selected as the main factors for quantifying crop area, with the influence of these factors determined based on feedback relationships. An increase in population and water supply drives the expansion of crop area, whereas GDP growth and technological advancement may enhance land use efficiency, thereby reducing the demand for crop area. The specific form is:

$$\frac{dA}{dt} = f(W_a) - f(TE) + f(P) - f(GDP) \quad (6)$$

$$A > A_{min} \quad (7)$$

where A is the crop area, A_{min} is the critical thresholds for crop area under land protection policies, W_a is the agricultural water use, other parameters meaning are the same as previously defined.

2.2.5. Environmental awareness equation

Environmental awareness reflects the perceived threat of system collapse by the community as the environment deteriorates. It tends to accumulate when the system performance falls below a critical threshold whereas it lapses otherwise (Van Emmerik et al., 2014). The dynamics of environmental awareness are influenced by both CO₂ emission rates and water scarcity. These factors concurrently enhance public awareness by capturing sensitivity to both long-term emission trends and water shortages. The use of CO₂ emission rates, as opposed to absolute values, more accurately reflects public risk perception, which is typically influenced by recent deterioration in environmental conditions.

This study adopts the conceptual framework proposed by Van Emmerik et al. (2014) to formulate community attitudes. The model structure is adapted from the community sensitivity equations developed by Chen et al. (2016) to better represent human responses to environmental changes. Additionally, the decay rate of regional environmental awareness is incorporated into the formulation, accounting for the gradual decline in concern once major environmental issues are perceived to be mitigated (Viglione et al., 2014). The specific form of the equation is shown as follows:

$$\frac{dE}{dt} = \frac{dCO_2}{dt} \times \frac{\nu_c}{CO_2} + \nu_r \times S - \mu \times E_{(t-1)} \quad (8)$$

where, E_t and $E_{(t-1)}$ represent environmental awareness at the current time period t and previous time period $t-1$, respectively, ν_c is the CO₂ emissions concern coefficient, ν_r is the water scarcity risk concern coefficient, μ represents the environmental awareness decay rate, where $\mu = 0.05$ when $E > 0$ and $\mu = 0.1$ when $E < 0$, S represents the water scarcity risk, other parameters meaning are the same as previously defined.

2.2.6. Water demand equation

Water demand is categorized into four sectors: domestic (DW_d), industrial (DW_i), agricultural (DW_a), and ecological water demand (DW_e). Each sector is influenced by population (P), GDP, crop area (A), green area (A_g), respectively, and jointly by available water supply and water price (P_r). Based on these factors, dynamic equations for water demand in each sector are established, and the total water demand is calculated as the sum of all sectors.

Since agricultural water use is difficult to be quantified directly, we assume that the actual regional water consumption is primarily influenced by the cultivation of major crops, which can be estimated as the product of crop area and actual evapotranspiration. Meanwhile, ecological water demand is mainly affected by green area and environmental awareness in urban regions. The specific form of the equation is shown as follows:

$$\frac{dDW}{dt} = \frac{dDW_d}{dt} + \frac{dDW_i}{dt} + \frac{dDW_a}{dt} + \frac{dDW_e}{dt} \quad (9)$$

$$\frac{dDW_d}{dt} = f(W_d) + f(P) - f(P_r) \quad (10)$$

$$\frac{dDW_i}{dt} = f(W_i) + f(GDP) - f(P_r) \quad (11)$$

$$\frac{dDW_a}{dt} = f(A \times ET_a) - f(P_r) \quad (12)$$

$$\frac{dDW_e}{dt} = f(A_g) + f(E) \quad (13)$$

where DW is total water demand. Furthermore, the Penman equation was used to calculate the potential evapotranspiration (ET_0) of crops, which was then multiplied by the crop coefficient (k_c) to obtain the actual evapotranspiration (ET_a) (Ji et al., 2025). The calculation formula is as follows:

$$ET_a = k_c \times \frac{0.408\delta(R_n - G) + \gamma \frac{900}{T+273} U_2(e_s - e_a)}{\delta + \gamma(1 + 0.34U_2)} \quad (14)$$

where, R_n is the net radiation at the crop surface ($MJ m^{-2} d^{-1}$); G denotes the soil heat flux ($MJ m^{-2} d^{-1}$), which is considered zero in this research; T is the average air temperature ($^{\circ}C$); U_2 represents wind speed at 2 m above the ground (m/s); e_s and e_a denote the saturation vapor pressure (kPa) and actual vapor pressure (kPa), respectively, δ is the slope of the saturation vapor pressure curve with respect to temperature (kPa/ $^{\circ}C$); and γ is the psychrometric constant (kPa/ $^{\circ}C$).

2.2.7. Auxiliary variables

Auxiliary functions play the critical roles in implementing feedback mechanisms among governing variables. These variables facilitate feedback control and enhance information transmission and dynamic responsiveness in the WEE coupling system (Pannocchia & Brambilla, 2007). Moreover, they support the formulation of constitutive relationships and contribute to the construction of mechanistic models, thereby enabling a more physically meaningful representation of

variable interactions. Auxiliary variables are selected and defined using two approaches: one based on physical mechanisms or mathematical formulas, and the other based on constitutive relationships.

(1) Water balance

The water balance equation represents the equilibrium between regional water inputs and outputs (Zhao et al., 2023). According to the water balance equation, the available water supply in the region is replenished by precipitation, inflows, and external water transfer.

$$W = \varphi R A_r + W_t \quad (15)$$

$$W = W_d + W_i + W_a + W_e \quad (16)$$

where W represents the total water use for four sectors: domestic (W_d), industrial (W_i), agricultural (W_a), and ecological (W_e), W_t is the available transferred water from the IBWT project, A_r is the total area of the research region (Km^2), R is the annual rainfall intensity, and φ is the runoff coefficient, which is set to be constant for simplicity. Because this is not the focus of our study, precipitation is assumed to be an independent input variable, while inflows and outflows remain constant annually, derived from historical observational data.

(2) Income

Disposable income (I) is calibrated and fitted from historical data to form a function of GDP and population. The specific formula is:

$$I = f(GDP/P) \quad (17)$$

(3) Technology

Technological advancements (TE), especially in agricultural irrigation, could enhance water use efficiency, reduce waste, and mitigate pollution, thus promoting long-term sustainability. In the model, TE is defined as an unobservable auxiliary variable that represents endogenous technological progress in resource efficiency, driven by the combined effects of economic growth, population, and environmental awareness.

$$TE = f(GDP, P, E) \quad (18)$$

(4) Green area

The green area (A_g) is calibrated using historical data and modeled as a function of ecological water demand and environmental awareness.

$$A_g = f(GDP) - f(A) \quad (19)$$

(5) Water scarcity risk

Water scarcity risk (S) is defined as the ratio of the supply–demand gap to water demand, with values ranging from -1 to 1 .

$$S = \frac{DW - W}{DW} \quad (20)$$

(6) Water price

Variations in water prices (P_r) primarily influenced the water scarcity and environmental awareness. In IBWT projects, water pricing requires special consideration, as transferred water typically costs more than locally sourced water (Liu et al., 2023). Therefore, a segmented water pricing function is constructed, prioritizing local over IBWT water supply. The specific formulation is as follows:

$$P_r = \begin{cases} f(S, E, W) & S > 0 \\ f(S, E, W_t, W_l) & S > 0 \& DW > W_l \\ f(S, E, W_l) & S < 0 \& DW < W_l \end{cases} \quad (21)$$

where W_l is the local water supply, W_t is the IBWT project water supply, other parameters meaning are the same as previously defined.

2.3. Constitutive relations

The constitutive relationship, expressed through differential equations, forms the foundation of system dynamics (Elshafei et al., 2014; Jia et al., 2021). It represents the inherent connections among variables in the coupled system to influence the system evolution. According to sketch of complex interconnections of WEE system, two types of relationships are considered herein to complete the dynamic system model: (1) Use mathematical or statistical methods to describe the interactions among different subsystems and quantify the relationships among variables. (2) Construct response functions by analyzing how changes in influencing variables contribute to the overall growth of governing variables. In the WEE coupling system, dependencies exist among governing, auxiliary, and driving variables. For example, the change in population growth rate is considered a function of temperature and domestic water supply. This implies that variations in temperature or domestic water supply will affect changes in the population growth rate.

The construction of response functions involves decomposing the total growth rate of the governing variables into multiple parts, each corresponding to a different factor. For a governing variable V with a total growth rate $O(V)$, modeling becomes more complex as $O(V)$ changes over time. To address this complexity, an annual average growth rate is applied to forecast future system states. The growth of V due to the specified response factor F_i can be expressed as follows:

$$I_{F_i}(V) = N_i(F_i) \times w_i(F_i) \times K_i(F_i) \times O(V) \quad (22)$$

where $N_i(F_i)$ is the sign function, showing the positive or negative effect of factor F_i :

$$N_i(F_i) = \begin{cases} 1 & \text{positive} \\ -1 & \text{negative} \end{cases} \quad (23)$$

The weight $w_i(F_i)$ represents the contribution of factor F_i to the growth of variable V , with these weights determined based on expert knowledge or observational data. Their total sum is constrained to 1, expressed as $\sum_{i=1}^N w_i(F_i) = 1$. The function $K_i(F_i)$ is used to normalize F_i within the range $[0,1]$.

2.4. Sensitivity analysis

Sensitivity analysis is conducted to evaluate how the SD model of the WEE coupling system responds to model parameters. A variance-based sensitivity analysis method has been widely applied in complex hydrological and ecological modeling (Van Emmerik et al., 2014; Yu et al., 2024). The computational procedure is as follows: First, parameter values are varied within a predefined range, with only one parameter adjusted at a time using uniform sampling within its respective range. These results are then compared with the best-fitting model output to compute the root mean squared error (RMSE) for each outcome variable. The variance of RMSEs, V_i , corresponding to the samples of parameter i is then calculated. Finally, the variances of RMSEs over the samples are then used to calculate the sensitiveness of model parameters (Sobol', 2001). The specific formulation is as follows:

$$S_i = \frac{V_i}{\sum_{i=1}^N V_i} \quad (24)$$

Table 1
Scenario design description.

Scenario	Input	Description
History (2002–2023)	Current development conditions	Model calibration and historical validation
Future (2024–2100)	Ensemble mean of ten SSP245 models Climate variables from each model under SSP245 and SSP585 scenarios Adjusted inter-basin water transfer capacities (50 % and 150 %)	Long-term trends under continued development trajectory Comparative assessment of climate change impacts on WEE system trajectories Evaluates how changes in inter-basin water transfer capacity affect the future evolution

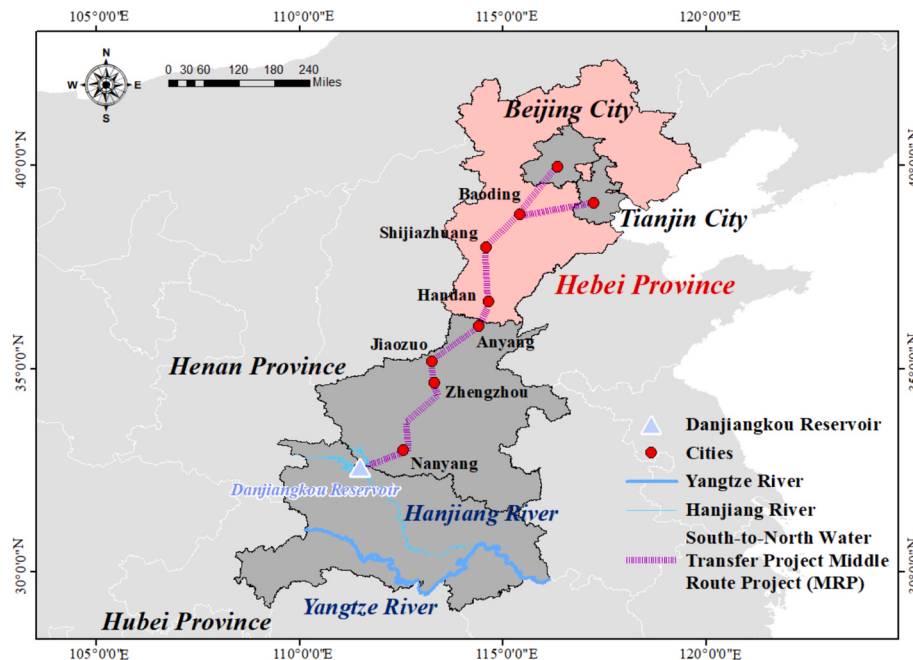


Fig. 3. Location of the South-to-North Water Transfer Middle Route Project.

where i is the tested parameter, N is the number of parameters ($i = 1, \dots, N$), V_i is the variance of RMSEs corresponding to parameter i , and S_i is the sensitivity index for the i th parameter.

In addition, the sensitivity of the proposed SD model to all the driving variables, including temperature, local water availability, and transferred water, is investigated to demonstrate the robustness of the proposed SD model. Specifically, each driving variable varies from 50 % to -50 % of the standard value with the step of 25 %, while keep other factors constant.

2.5. Scenario design

This study establishes four scenario settings (Table 1) to assess the evolution of the WEE system in the IBWT water-receiving areas with the impacts of climate change and the water transfer capacities. The first scenario simulates the historical phase of the WEE system using current development conditions and designed amount of transferred water. It serves primarily for model validation and to characterize the baseline dynamics of key state variables. The second scenario incorporates the ensemble average of temperature, precipitation, and other climate variables from ten SSP245 models as external inputs. This scenario represents a continuation of current development trends and is used to explore the system's long-term evolutionary patterns, periodic behavior, and potential emerging phenomena. To further investigate the impacts of climate change, the third scenario compares the SSP585 with the SSP245 to investigate the differential effects of future climate change on the WEE system's trajectories. Finally, to examine the influence of water

transfer capacities under future conditions, the amount of transferred water is adjusted to 50 % and 150 % of the current planned levels in both SSP245 and SSP585 scenarios.

3. Case study

3.1. Study area

Water resources in China exhibit significant spatial heterogeneity. The annual water availability per capita in Northern China (~910 m³/year) is significantly lower than that in the south (~3,180 m³/year) (Ministry of Water Resources of China, 2018). Rapid urbanization in northern regions has further intensified water scarcity. To address this challenge, the South-to-North Water Transfer Middle Route Project (MRP) was implemented to divert water from the Han River Basin, a water-abundant region in the south, to the water-deficient North China Plain. The MRP began transferring water to northern China in December 2014, with an annual diversion capacity exceeding 9.5 billion m³. The project originates from the Danjiangkou Reservoir in Hubei Province and extends along the western edge of the Yellow River-Huaihe River-Haihe River Plain, passing through Henan, Hebei, Beijing, and Tianjin. It provides essential water resources for domestic, industrial, ecological, and partial agricultural use in these regions (Long et al., 2024). Fig. 3 shows a schematic diagram of the project.

This study selects Hebei Province, one of the water-receiving areas of the MRP, as the primary research region. As of 2023, the study area covers a total of 188,800 square kilometers, has a population of 73.93 million, and contributes 4.2 % to the national GDP. According to the

Table 2

Introduction of the datasets used in this study.

Data	Sources
GDP	National Bureau of Statistics of China
Green area	
Population	Hebei Province Statistical Yearbook
Crop area	
Water demand	Hebei Province Water Resources Bulletin
CO ₂ emission	Calculated from (Ji et al., 2025) based on China Energy Statistics Yearbook
Historical meteorological data	CN05.1 dataset
Future meteorological data	Coupled Model Intercomparison Project Phase 6

Table 3

Initial setting of the six governing variables including population (P), GDP, CO₂ emissions (CO_2), crop area (A), environmental awareness (E), water demand (DW). Three driving variables including temperature (T), local water supply (W_l) and water transfer (W_t).

Variables	Unit	Eq.	Initial value
Population (P)	1×10^4 people	(1–3)	6735.0
GDP	1×10^8 RMB	(4)	5518.9
CO ₂ emissions (CO_2)	1×10^4 tons	(5)	16521.4
Crop area (A)	1×10^3 ha	(6)	8935.1
Water demand (DW)	$1 \times 10^8 m^3$	(9)	211.39
Temperature (T)	°C	–	11.93
Local water supply (W_l)	$1 \times 10^8 m^3$	(–)	210.51
Water transfer (W_t)	$1 \times 10^8 m^3$	(–)	0
Environmental awareness (E)	–	(8)	0

project plan, Hebei Province is expected to receive an annual water allocation of 3.47 billion m³ (36.5 %) to alleviate the depletion of surface water resources and the continuous decline in groundwater levels driven by urbanization and agricultural practices (Hebei Provincial Bureau of Statistics, 2023). Furthermore, the project plans to further increase the water transfer to Hebei Province through the Yangtze River to Han River Water Transfer Project in the future, ensuring the sustainable supply of regional water resources (Xu et al., 2023).

3.2. Data description

The data are primarily categorized into socioeconomic data and meteorological data that drive the model's operation, as shown in Table 2. Economic system data for Hebei Province from 2002 to 2023, including population, GDP, and crop area, were obtained from the China Statistical Yearbook and Hebei Provincial Statistical Yearbook (<https://data.cnki.net/>). Historical water consumption data were sourced from the Hebei Provincial Water Resources Bulletin (<https://slt.hebei.gov.cn/>). The water transfer capacity and actual water distribution data (2014–2023) are sourced from the South-to-North Water Transfer Central Route Bureau. CO₂ emission data (2002–2023) were directly adopted from Ji et al. (2025), which were calculated based on the China Energy Statistical Yearbook (<https://www.stats.gov.cn/hd/lyzx/zxgk/nytj/>).

In this study, the CN05.1 dataset was used to provide historical meteorological data, including precipitation, evapotranspiration and temperature, for the period from 2002 to 2023. This dataset was generated by interpolating observational data from 2400 meteorological stations across China into grid points with a spatial resolution of 0.25° × 0.25° (Wu & Gao, 2013). The interpolation process employed the thin-plate smoothing splines method combined with angular distance weighting.

Future meteorological projections data were derived from the Coupled Model Intercomparison Project Phase 6 (CMIP6) outputs. The use of multiple Global Climate Models (GCMs) is essential to improve

Table 4

Calibrated constitutive relations needed to complete model specification.

Variables	Function
Population growth rate (r)	$-e^{-0.1T} + 10e^{7.5 \times 10^{-3}W_d} - 4$
Population carrying capacity (K_0)	$-6.5E - 5.2 \times 10^3 e^{0.001T} + 6.5 \times 10^3 e^{0.12W_d}$
Economic equation (GDP)	$2^{-2} \times e^{24 \times 10^3 P} \times e^{0.02E} \times e^{4 \times 10^3 W_l}$
CO ₂ emission (CO_2)	$5 \cdot 4e^{-0.1Ag} + 40e^{-TE} \cdot e^{1 \times 10^{-4}I} + 7e^{0.7T}$
Crop area (A)	$5e^{-5 \times 10^{-5}P} \cdot 15e^{-0.001GDP} + 2W_a^{0.5} + 2500(0.8 - e^{-0.1TE})$
Domestic water demand (DW_d)	$0.013 W_d - 1.5 \times 10^{-5} P \times W_d + 1 \times 10^{-5} W_p$
Industry water demand (DW_i)	$-0.15W_l \times GDP + W_p \times e^{-0.006W_l}$
Agricultural water demand (DW_a)	$1 \cdot 2e^{-0.1Ag} + e^{0.1E}$
Ecological water demand (DW_e)	$0.04A \times ET_a + e^{0.1W_p} - 1$
Income (I)	$(1 - e^{-0.1GDP/P}) \times 70,000$
Technology (TE)	$(2.4e^{0.00001GDP} + 2.6e^{0.00001P}) \times (1 - e^E)$
Green area (A_g)	$14e^{0.00003GDP} \cdot e^{0.0001A}$
Water price (P_r)	$\begin{cases} e^S + e^E + e^{0.001W_l} & S > 0 \\ e^S + e^E + e^{0.001W_t} + 0.5e^{0.001W_t} & S > 0 \& DW > W_l \\ e^S + e^E + 0.5e^{0.001W_t} & S < 0 \& DW < W_l \end{cases}$

Table 5

The ranges of parameters tested in the sensitivity analysis.

Variables	Unit	Eq.	Value	Min.	Max.	Description
r_0	%	1	8	8	15	Basic population growth rate
α_1	%	1	-1	-1	5	Temperature growth rate parameter
α_2	%	1	10	10	20	Water supply growth rate parameter
K_0	10^4	1	6500	6500	7000	Environmental carrying capacity
β_1	10^4	1	-6.5	-10	0	Domestic water carrying capacity parameter
β_2	10^4	1	6500	6500	7500	Income carrying capacity parameter
β_3	10^4	1	-5200	5200	-4800	Environmental awareness carrying capacity parameter
χ	–	3	-3	-3.5	-2.9	Population elasticity coefficient
δ	–	3	-2	-2.0	0	Water resource elasticity coefficient
ε	–	3	2	2	2.5	Environmental elasticity coefficient
ν_c	–	7	0.1	0.05	0.2	CO ₂ emission concern coefficient
ν_r	–	7	0.1	0.05	0.1	Water scarcity risk concern coefficient
μ_c	–	7	0.05	0	0.2	CO ₂ emission awareness decay rate
μ_r	–	7	0.1	0.1	0.1	Environmental awareness decay rate

prediction reliability. Ten CMIP6 models under the SSP245 and SSP585 scenarios were selected for this study: ACCESS-ESM1-5, BCC-CSM2-MR, CESM2, EC-Earth3, GFDL-ESM4, HadGEM3-GC31-LL, MIROC6, MPI-ESM1-2-LR, MRI-ESM2-0, and NorESM2-MM. These models have shown high accuracy in replicating historical precipitation and temperature patterns (Zhang et al., 2021). The data are accessible through the World Climate Research Project (<https://esgf-node.llnl.gov/projects/cmip6/>).

3.3. Initial and boundary conditions

The observations of governing and driving variables in 2002 were set

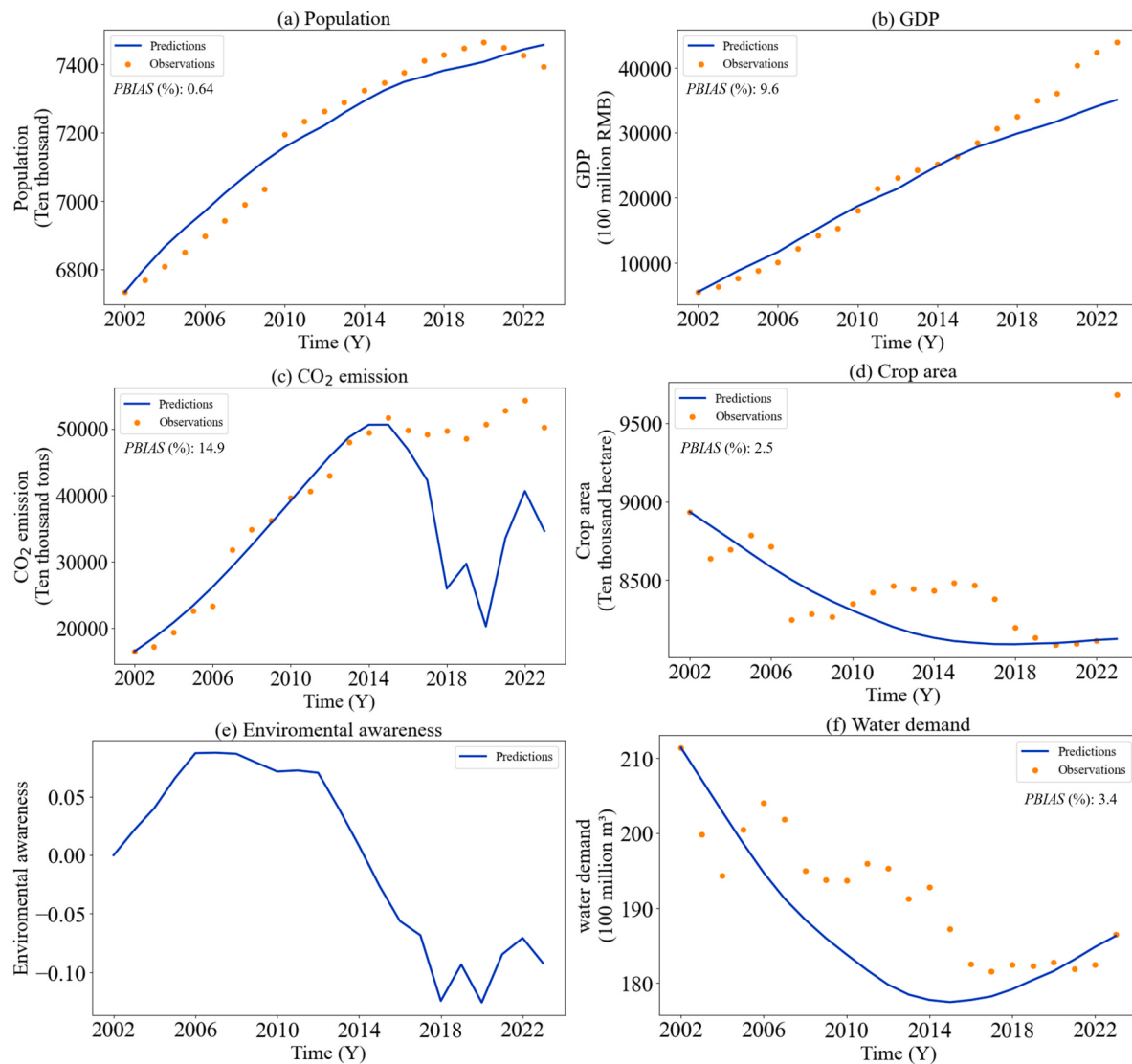


Fig. 4. Model validation of governing variables.

as the initial values of the SD model (Table 3). A simple explicit numerical scheme was adopted to solve the coupled system of differential equations at annual scale. Subsequently, Table 4 presents all the constitutive relationships obtained through trial-and-error calibration and validation using the WEE system conceptual model and data from the MRP water-receiving areas in Hebei. Table 5 defines the parameter values used in model construction and their specified ranges.

The parameter settings were determined following the traditional design in the existing research, and the optimal parameters were determined through trial and error. Observable parameters (e.g., population basic growth rate r_0 , environmental carrying capacity K_0) were derived from the Statistical Yearbooks, whereas the parameters related to environmental awareness were adapted from previous socio-hydrological studies (Chen et al., 2016; Elshafei et al., 2014; Van Emmerik et al., 2014). Other parameters, such as growth rate parameter and elasticity coefficient, were adjusted based on system behavior until simulated trajectories matched historical records. The SD model aims to capture broader patterns in model trends and derive generalizable insights that may be applicable to other regions (Van Emmerik et al., 2014).

4. Results and discussion

4.1. Model validation

Figs. 4 and 5 indicated that the model simulations of governing and auxiliary variables matched well with the observations. The PBIAS of all governing variables fall within the range of $\pm 20\%$ (acceptable level of accuracy) during the historical period from 2002 to 2023, demonstrating the reliability of the proposed SD model. In addition, the coefficients of determination (R^2) are generally above 0.5, with those of the economic subsystem showing superior performance, all exceeding 0.9. Most of the Nash-Sutcliffe Efficiency (NSE) coefficients fall within the acceptable range, while a few NSE values are below zero, primarily due to limitations in historical data. Nevertheless, the simulated evolutionary trends of the indicators are considered reasonable; therefore, the simulation results are deemed acceptable, as shown in Table 6.

For the historical evolution of the economy subsystem in the Hebei regions, the population and GDP maintained growth trajectories with the decreasing growth rates (Figs. 4a and 4b), and the per capita disposable income exhibited a steady upward trend. Concurrently, crop area has been steadily decreased to critical thresholds due to urbanization (Fig. 4d). In the environment subsystem, environmental awareness rose significantly in response to the rapid increase in CO₂ emissions

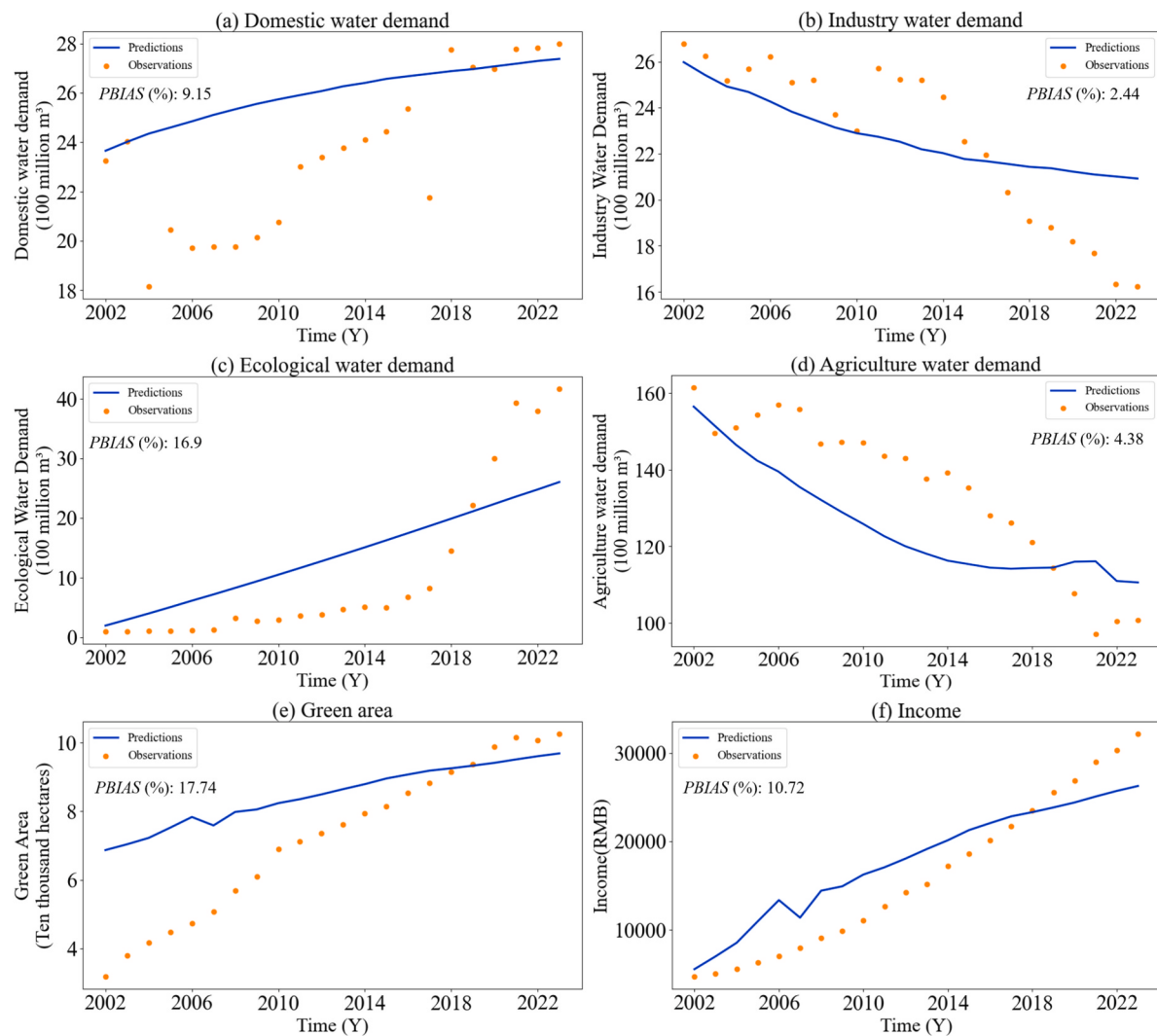


Fig. 5. Model validation of selected auxiliary variables.

Table 6
Performance metrics for assessing the system dynamics model.

Variables	PBIAS (%)	R ²	NSE
Population (P)	0.64	0.97	0.95
GDP	9.64	0.97	0.91
CO ₂ emissions (CO ₂)	14.9	0.44	-0.06
Crop area (A)	1.8	0.57	0.29
Water demand (DW)	3.4	0.55	0.01
Domestic water demand (DW _d)	9.15	0.52	-0.09
Industry water demand (DW _i)	2.44	0.67	0.52
Ecological water demand (DW _e)	16.9	0.73	0.62
Agriculture water demand (DW _a)	4.38	0.62	0.52
Green area (GA)	17.74	0.98	0.28
Income (I)	10.72	0.91	0.81

observed prior to 2014 (Figs. 4c and 4e), while green space area also expanded rapidly. Environmental awareness is an unobservable latent variable that reflects public attitudes toward environmental change. Results indicated that higher environmental awareness generally emerges under increased CO₂ emissions and water stress, consistent with observed environmental trends, indicating a reasonable representation of social responses. It should be noted that there is a divergence in CO₂ emissions during the period after 2015. The divergence arises because the historical emissions, estimated based on the China Energy Statistics Yearbook and sectoral emission factors, didn't account for ecological

carbon sinks, resulting in higher values than those simulated by the model. As shown in Fig. 5c, ecological water use has increased substantially since 2015, generating a noticeable carbon sink effect in the model and leading to a further divergence between two datasets in the later period. In addition, the simulation accuracy is limited because the coupled human–nature WEE system cannot fully capture the complexity of the carbon cycle, such as the simplification of land-use change and ecological feedbacks, as well as assumptions regarding socioeconomic pathways and feedback mechanisms (Morris et al., 2025; Ramanathan et al., 2021). Nevertheless, the simulated evolutionary trends are generally consistent with the historical observations, demonstrating that the SD model effectively captures the future trajectory of the WEE system (Feng et al., 2016; Jia et al., 2021).

Water demand reached a significant turning point during 2014–2015 due to the MRP project, followed by a consistent upward trend (Fig. 4f). Both domestic and ecological water demand continue to rise (Figs. 5a and 5c). However, under the influence of water district policy regulations, industrial water and agricultural water demands show a decreasing trend (Figs. 5b and 5d). Technological advancement exhibited a generally stable upward trajectory, ranging from 1.6 to 2.5 throughout the study period (Fig. S1). Notable accelerations were observed around 2006 and 2020, corresponding to major economic restructuring and policy-driven transitions in the study area.

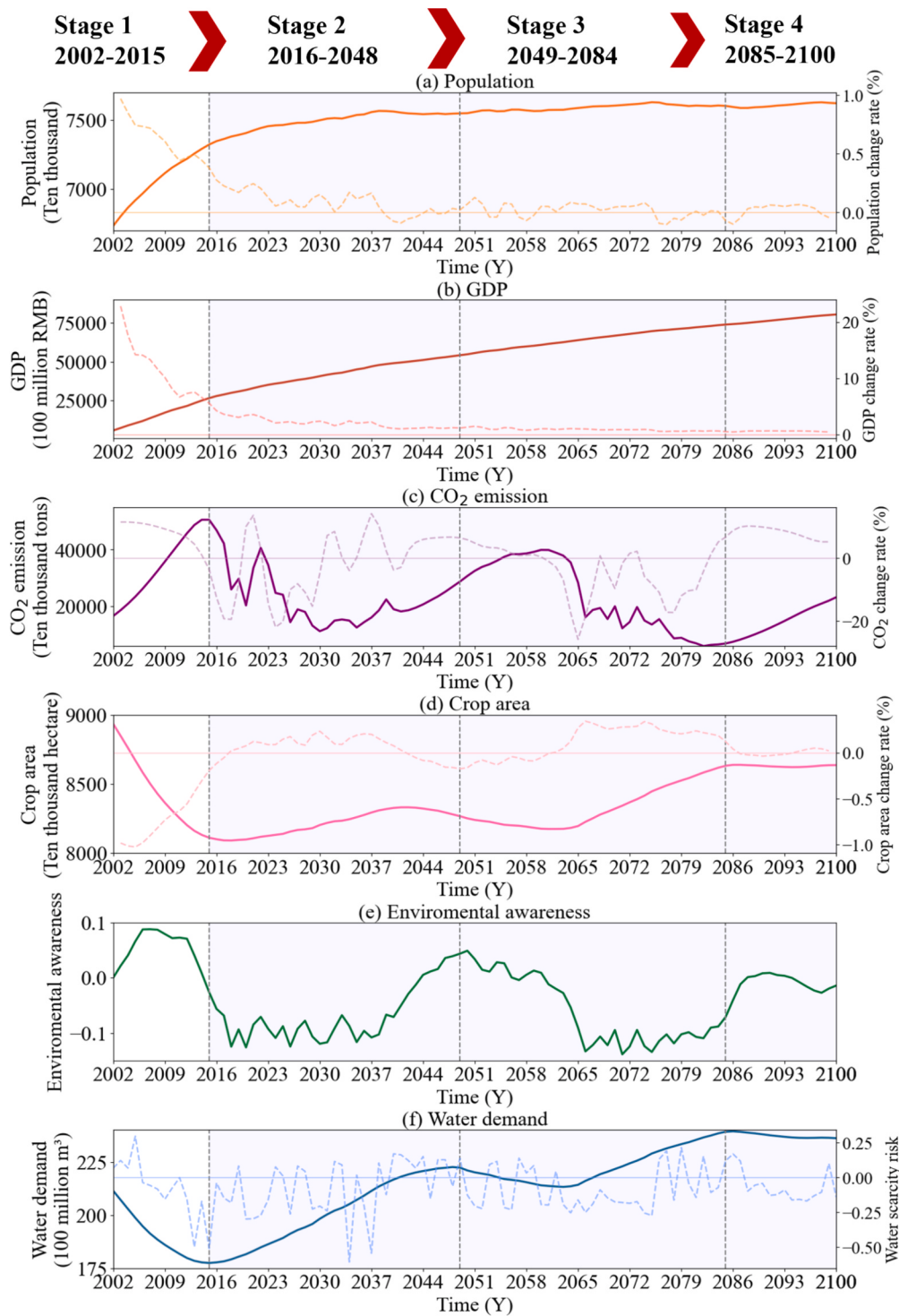


Fig. 6. Evolution process of six governing variables in the WEE system during the time period from 2002 to 2100. The time period with blue background represents the period with MRP project implementation since Dec 2014. Solid lines correspond to the primary y-axis, while dashed lines represent variables plotted on the secondary y-axis. (For interpretation of the references to colour in this figure legend, the reader is referred to the web version of this article.)

4.2. Evolution of the WEE system in the future

The evolution process of the WEE coupling system is divided into four stages (Fig. 6) based on the slopes of total water demand changes (rates are 0 in Fig. S2), which generally aligns with the urban evolution process of expansion (stage 1 from 2002 to 2015), degradation (stage 2 from 2016 to 2048), recovery (stage 3 from 2049 to 2084), and stability (stage 4 from 2085 to 2100) (Feng et al., 2016). Stage 1 refers to the

historical data, which is defined as the trend of expansion (more details in Sect. 4.1).

Stage 2 is characterized by a period of degradation, during which both population and GDP growth decelerate, with the population even experiencing negative growth for the first time (Fig. s. 6a and S3). This indicates a transition toward a development model that prioritizes quality and efficiency. CO₂ emissions decline due to economic restructuring and policy incentives under conditions of slower GDP and

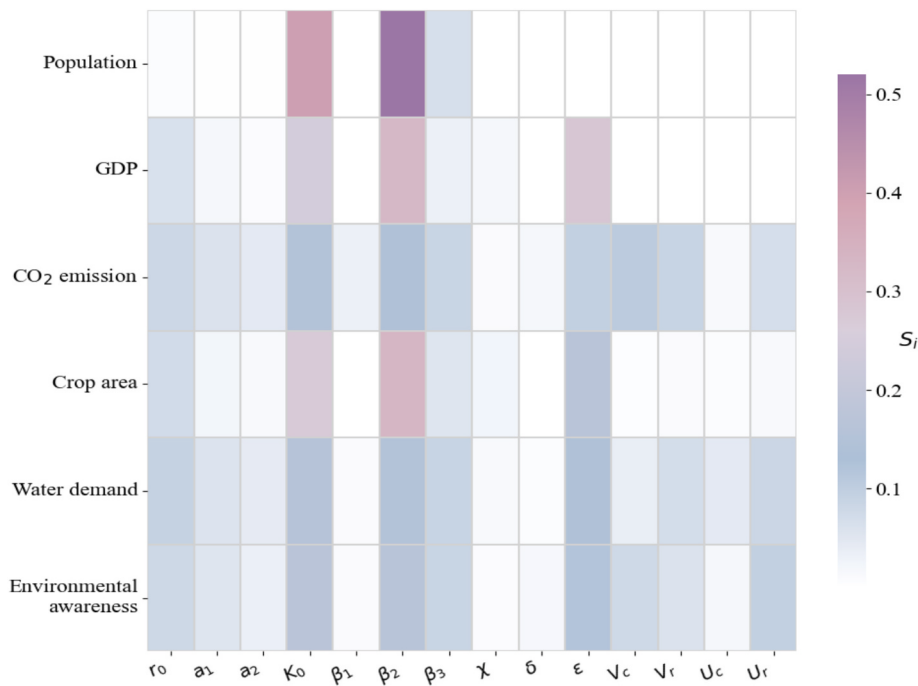


Fig. 7. Sensitivity index (S_i) of all model parameters to the governing variables. The color bar indicates the magnitude of the S_i , with deeper shades representing a stronger influence of the parameter on the governing variable.

population growth. Meanwhile, cropland area stabilizes as a result of land protection policies enforcing minimum cultivated area requirements. The environmental awareness fluctuates at low level and then increases under the combined effects of increased CO_2 emissions change rates and water scarcity risk. Water demand exhibits variable growth, influenced by MRP and ecological strategies, with increasing emphasis on ecological water requirements.

Stage 3 begins in 2049, marking a period of system recovery. Although population growth shows a mild rebound, negative growth rates still occur intermittently (Fig. 6a and S2). In contrast, GDP growth remains relatively stable with modest increases, indicating the consolidation of a mature and resilient economic structure. Driven by a renewed increase in population growth, crop area expands again to address growing food demand and enhance regional food security. Despite a noticeable rebound in the early stages, CO_2 emissions exhibit an overall declining trajectory, driven by structural economic transitions and technological advancements that collectively reflect the sustained effectiveness of low-carbon policies. These temporal rebounds of CO_2 emissions rates renew public environmental awareness, underscoring the critical role of environmental governance. Meanwhile, water demand tends to stabilize with modest growth, indicating that the WEE coupling system reaches its peak water demand at the end of stage 3. At this stage, with economic development stabilizing, both environmental awareness and climate change increasingly shape the trajectories of carbon emissions and water demand.

In Stage 4, the WEE coupling system enters a new phase of evolution and stability, as the governing variables reach a new equilibrium following Stage 3. The magnitude of changes across variables becomes minimal, indicating system convergence. However, the sustainability and long-term implications of this stabilization remain to be further validated and optimized under diverse future scenarios.

CO_2 emissions have already peaked in 2016, marking the achievement of carbon peaking within the WEE system. This peak arises from the model's endogenous economic-environmental feedback mechanisms and should not be interpreted as an actual policy-driven outcome. In contrast, water demand, driven by continued population growth and economic expansion, is expected to increase significantly until 2049.

Thereafter, factors such as climate change, ecological restoration initiatives, and the implementation of the IBWT project may alter demand trajectories, with a potential peak projected around 2085. These drivers may also induce a rebound in CO_2 emissions, potentially postponing the minimum of carbon emissions in approximately 2085. Notably, carbon emissions remain highly sensitive to shifts in public environmental awareness, and could easily rise again under continued socioeconomic development.

4.3. Model sensitivity and robustness

Fig. 7 demonstrates the overall robustness of the proposed SD model, with notable sensitivity to environmental carrying capacity (k_0), income carrying capacity parameter (β_2), and environmental elasticity coefficient (ε). Both the income carrying capacity coefficient (β_2) and the environmental carrying capacity coefficient (k_0) originate from the carrying capacity terms in the population growth equation (Equation (3)) and directly regulate the rate of population growth. As a fundamental component of the system, the population growth rate not only significantly impacts major governing variables in the economic subsystem (e.g., GDP and crop area), but also influences other subsystem variables through multiple feedback mechanisms. The environmental elasticity coefficient (ε) in the GDP growth rate equation (Eq. (4)) characterizes the regulatory effect of environmental awareness on economic growth. The model's high sensitivity to this parameter underscores the critical role of environmental awareness in modulating the pace of economic development. Given the structural design of the model, population shows limited sensitivity to ε , as environmental awareness primarily influences economic rather than demographic processes. In contrast, ε exerts influence on other governing variables either directly or indirectly through economic linkages, thereby emphasizing the pivotal role of environmental awareness in shaping overall system behavior. Fig. 8 and S4 show that parameter changes affect only the magnitude, not the trajectory, of governing variable evolution. The most pronounced effects occur in Stages 2 and 3, which represent critical transition periods where cumulative parameter impacts intensify until reaching either resource carrying capacity or model-imposed limits.

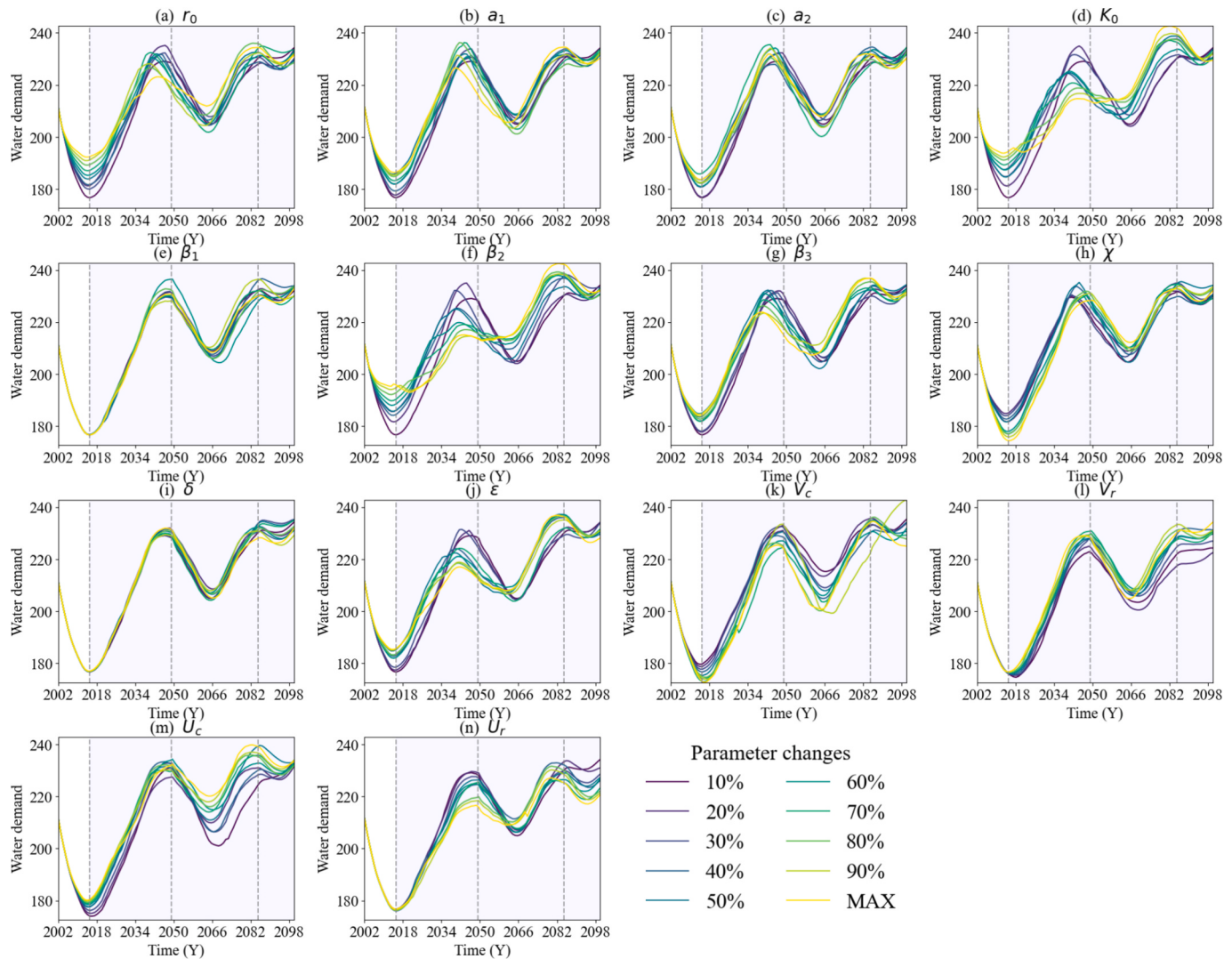


Fig. 8. Variations of total water demand under varying model parameters from minimum to maximum with the step of 10%. The background colors are consistent with Fig. 6.

The governing variables have different sensitivity to the key driving variables, including temperature, local water supply, and the amount of transferred water (Fig. 9). Specifically, temperature has relatively minor effects in Stage 1 and 2, but its influence on carbon emissions, water demand, and crop area increases in Stages 3 and 4. This shift arises from the dominance of rapid population and GDP growth during the early stages, which exceeds the influence of climatic variables on system dynamics. As these socio-economic drivers stabilize in Stages 3 and 4, their contributions to system variability diminish, rendering the system increasingly sensitive to climatic perturbations. In contrast, water availability exerts a more pronounced impact on the evolution of the WEE coupling system. Local water supply affects both the fluctuation range and trajectories of governing variables, while transferred water primarily regulates the amplitude of governing variables. These two factors play a dominant role in shaping the evolution of the WEE coupling system in Hebei regions. Accordingly, the availability of water resources, particularly the transferred water via the MRP, emerges as a critical driver for forecasting socioeconomic dynamics and the peak timings of water demand and carbon emissions.

4.4. Impacts of climate change on the evolution of the WEE system

Fig. 10 illustrates the projected variations of governing variables

under climate change for the SSP245 and SSP585 scenarios during the period 2016–2100, while Fig. S5 compares their performance across ten distinct models. Specifically, population and GDP exhibit more rapid growth under SSP585 than SSP245 scenarios, with accelerated population expansion in SSP585 driving increased food demand and a corresponding increase in crop area. Under this high-emission scenario, CO₂ emissions remain elevated and environmental awareness is relatively low, posing greater challenges for achieving emission reduction targets compared to SSP 245 scenario. Water demand exhibits a steeper upward trajectory under SSP585, with its peak occurring later compared to SSP245. Results highlight a strong linkage between climate policies and sustainable development goals across different socioeconomic pathways. High-emission SSP585 scenario promotes economic growth but intensifies resource competition and environmental degradation, whereas moderate-to-low SSP245 emission scenario offer a more balanced approach by aligning development goals with ecological constraints.

Fig. 11 shows that increasing MRP transfer capacity significantly accelerates the growth of population, GDP, crop area, and water demand under both SSP245 and SSP585 scenarios. While enhanced MRP transfer capacity supports the development of both economy and water resource subsystems, its impacts on carbon emissions and environmental awareness are relatively more complex. Overall, current MRP transfer

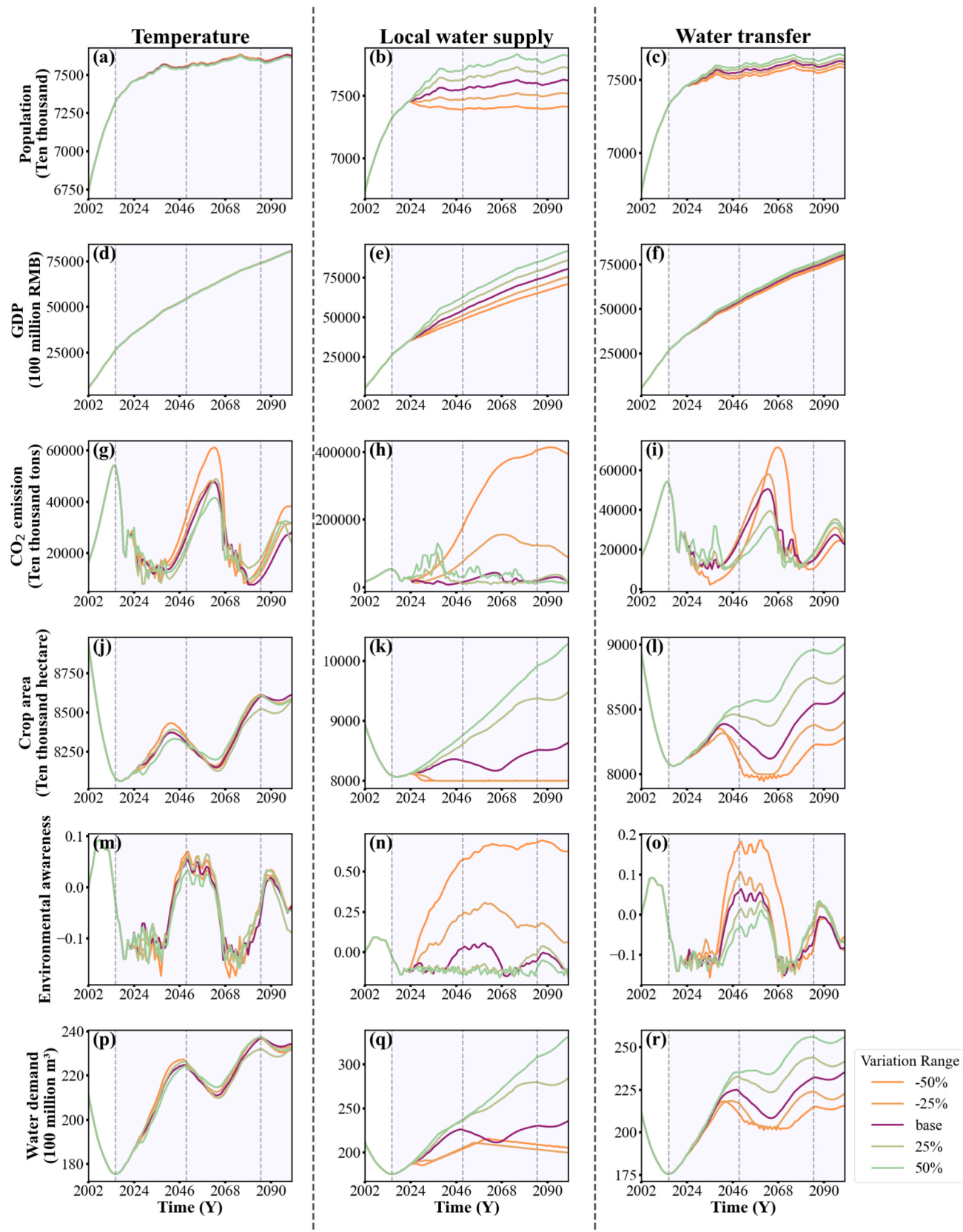


Fig. 9. Trajectories of governing variables with varied driving variables. Three driving variables are adjusted by increasing or decreasing by 25% and 50% based on their standard values, while keeping others constant. The color of the background and the meaning of the dotted lines are consistent with fig. 6.

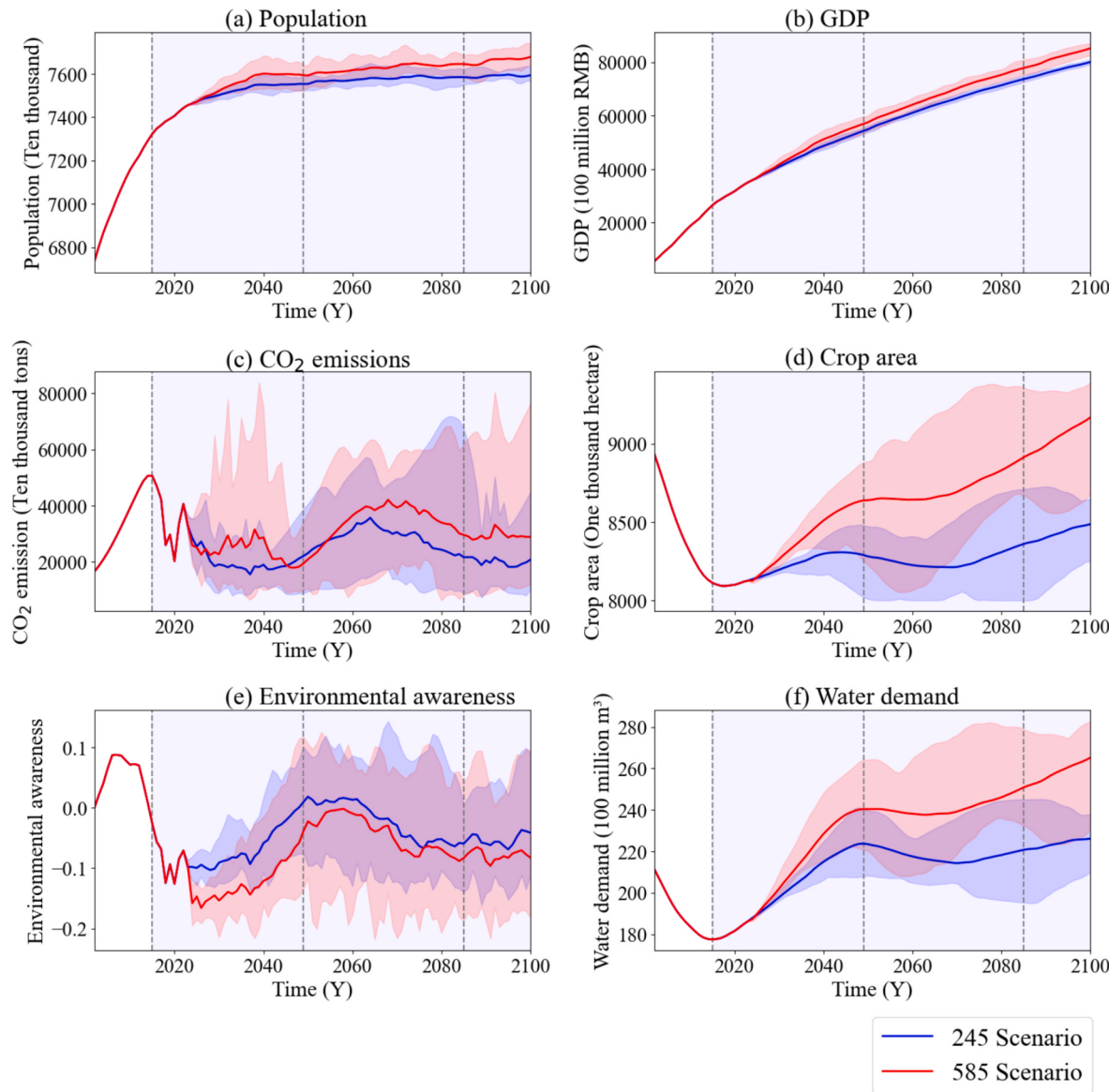


Fig. 10. Trajectories of governing variables under SSP 245 and 585 scenarios during the period from 2016 to 2100. The bold lines represent the ensemble mean of 10 CMIP6 models, while the shades denote one standard deviation between these models. The background colors are consistent with fig. 6.

capacity appears to be more effective in achieving energy conservation and emission reduction targets. Notably, expanded water transfer capacity leads to a marked decline in carbon emissions and environmental awareness under both SSP245 and SSP585 scenarios in Stage 3 (recovery). This is primarily due to renewed economic development, which increases water resource demand (ICGEM, 2018). Enhanced transfer capacity helps stabilize the supply–demand balance, thereby improving overall system efficiency and reducing dependence on energy-intensive water use (Griffiths-Sattenspiel & Wilson, 2009). Meanwhile, improved water availability and lower carbon emissions may lead to a decline in public environmental awareness. However, in Stage 2 (degradation), when economic growth slows, additional MRP water transfer may impose economic burden without delivering proportional environmental benefits. In stage 4 (stability), as the system approaches a balanced state of water supply and demand, most of the extra water is allocated to low-priority uses such as urban greening and domestic consumption rather than replacing high-carbon water sources. Consequently, the effectiveness of transfer expansion in reducing emissions diminishes during Stages 2 and 4. Moreover, increased water transfer capacity often alleviates water stress in Hebei regions, which may

reduce residents' environmental awareness and dampen their motivation for sustainable water use.

5. Implications and limitations

The SD modeling and key insights from this study are transferable to other IBWT-receiving areas with similar socio-environmental conditions. The findings indicate that the future evolution of the WEE coupled system in water-receiving areas will be jointly influenced by both climate change and water resource availability, exhibiting periodic fluctuations over time. Among these factors, water availability exerts the most pronounced influence, highlighting the pivotal role of IBWT projects in controlling regional WEE system evolution. Furthermore, the economy subsystem emerges as the dominant driver within the WEE framework. Notably, improvements in public environmental awareness exerts a substantial influence on the long-term trajectory of the WEE system, underscoring the importance of incorporating socio-behavioral dimensions into future planning efforts. Based on these findings, we propose the following recommendations: (1) Given the cyclical nature of WEE system evolution and the risk of carbon emission rebound, it is

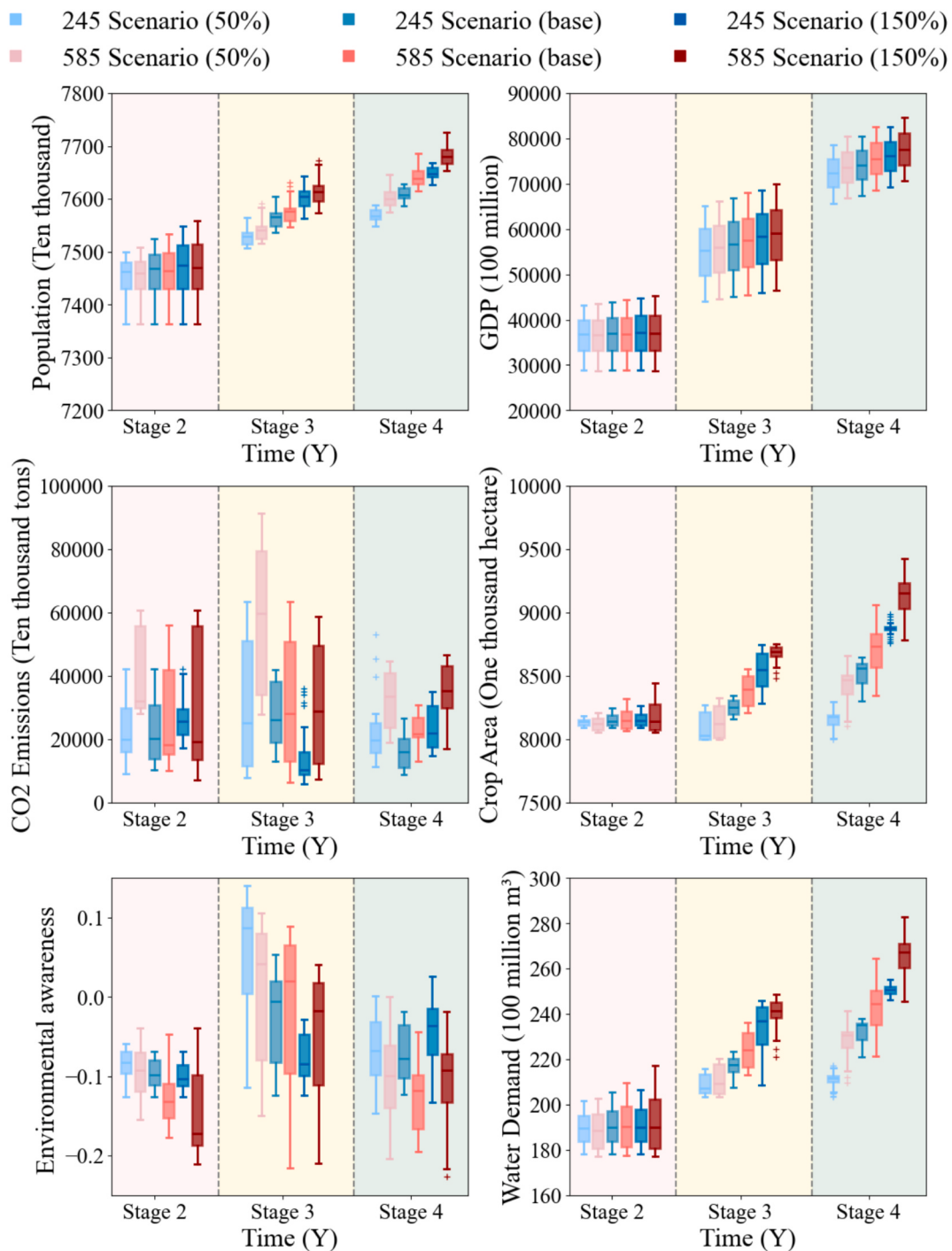


Fig. 11. Impact of the amount of transferred water on governing variables at different stages under SSP 245 and 585 scenarios. The blue box represents the SSP245 scenario, while the red box represents SSP585. The color gradient from light to dark indicates 50%, 100%, and 150% of the planned amount of transferred water. The red, yellow, and blue backgrounds correspond to future development stages 2, 3, and 4, respectively. (For interpretation of the references to colour in this figure legend, the reader is referred to the web version of this article.)

crucial to implement emission control strategies during the recovery phase to prevent post-stabilization surges. (2) The necessity of IBWT is reaffirmed, but IBWT management must be aligned with evolving system demands. It requires decision-makers to balance resource availability and economic growth through well-planned adjustments in water transfer capacities. (3) Adopting low-emission development pathways, such as those represented by SSP245, rather than prioritizing rapid economic expansion, can alleviate future pressures on water, food, and environment systems. (4) Strengthening public environmental

awareness is essential for promoting energy and water conservation and enhancing the effectiveness of sustainability policies.

However, there are some limitations that warrant further investigation: (1) The model does not fully account for complex CO₂ fluxes, such as carbon stock in the ecosystems. (2) The current model excludes population migration and adaptive water management strategies, which may significantly affect future dynamics. Future studies should incorporate diverse governance scenarios, such as water pricing adjustments and water rights trading, to enhance policy resilience under varying

climate conditions.

6. Conclusions

This study developed an integrated system dynamics (SD) framework to investigate the long-term evolution of the water–economy–environment (WEE) coupling system in inter-basin water transfer (IBWT) receiving regions. The framework was applied to the Hebei province, a major water-receiving region of China's South-to-North Water Transfer Middle Route Project (MRP). Our major findings include:

- (1) The coupled nonlinear ordinary differential equations embedded in the SD model effectively capture the interdependencies within the regional WEE system, achieving PBIAS values within $\pm 20\%$ for the governing variables, demonstrating strong robustness. This approach provides a reliable tool for exploring the dynamic feedback behaviors in WEE subsystem interactions and shows potential for generalization to other IBWT receiving areas.
- (2) The evolution of the WEE coupling system can be categorized into four distinct stages: expansion, degradation, recovery, and stability. Under the influence of climate change, the environment and water resource subsystems remain highly sensitive, resulting in CO₂ emissions and water demand peaking in 2016 and 2085, respectively. Notably, carbon emissions are strongly influenced by environmental awareness, often exhibiting rebound effects when regulatory pressure weakens.
- (3) The SSP245 scenario aligns more closely with sustainable development goals among the simulated scenarios. Enhanced IBWT capacity promotes economic recovery and indirectly reduces CO₂ emissions by stabilizing the water supply–demand balance and decreasing dependence on energy-intensive water use. However, determining the optimal water transfer capacity requires policymakers to balance between economic development and resource conservation objectives, underscoring the need for adaptive policy decisions.

In summary, the proposed system dynamics approach can effectively capture the evolution of the WEE coupling system in IBWT water-receiving areas. The findings provide quantitative insights to support sustainable water resource management and inform adaptive policy formulation under future climatic and socio-economic uncertainties.

CRediT authorship contribution statement

Danni Jia: Writing – original draft, Validation, Software, Methodology, Formal analysis, Data curation, Conceptualization. **Jingwen Zhang:** Writing – review & editing, Validation, Supervision, Project administration, Methodology, Funding acquisition, Conceptualization. **Zejun Li:** Supervision. **Maoyuan Feng:** Writing – review & editing, Supervision. **Kairong Lin:** Supervision. **Xiaohong Chen:** Supervision. **Xiaohui Lei:** Supervision. **Lixin He:** Supervision. **Chao Ma:** Supervision. **Jingru Ji:** Data curation.

Declaration of competing interest

The authors declare that they have no known competing financial interests or personal relationships that could have appeared to influence the work reported in this paper.

Acknowledgments

This research has been supported by the National Key R&D Program of China (2023YFC3209400, 2023YFC3209401-03), the National Natural Science Foundation of China (52479034, 52309014), the Fundamental Research Funds for the Central Universities, Sun Yat-sen University (23hytd011), Guangdong Basic and Applied Basic Research

Foundation (2024A1515010968), and Science and Technology Innovation Program from Water Resources of Guangdong Province (2024-04).

Code and data availability

The socioeconomic and meteorological data used in this study are publicly available from the following sources: China Statistical Yearbook and Hebei Provincial Statistical Yearbook (<https://data.cnki.net/>), Hebei Provincial Water Resources Bulletin (<http://slt.hebei.gov.cn/>), China Energy Statistical Yearbook (<http://www.stats.gov.cn/hd/lyzx/zxgk/nytj/>), historical meteorological data from the CN05.1 dataset (Wu & Gao, 2013), and future climate projections from CMIP6 models accessible via the World Climate Research Project (<https://esgf-node.llnl.gov/projects/cmip6/>). The code supporting the findings of this study is available from the corresponding author upon reasonable request.

Appendix A. Supplementary data

Supplementary data to this article can be found online at <https://doi.org/10.1016/j.jhydrol.2025.134732>.

Data availability

Data will be made available on request.

References

- Abolghasemzadeh, H., Zekri, E., Nasseri, M., 2024. Regional-scale energy-water nexus framework to assess the GHG emissions under climate change and development scenarios via system dynamics approach. *Sustain. Cities Soc.* 111, 105565. <https://doi.org/10.1016/j.scs.2024.105565>.
- Almulhim, A.I., Alverio, G.N., Sharifi, A., Shaw, R., Huq, S., Mahmud, M.J., Ahmad, S., Abubakar, I.R., 2024. Climate-induced migration in the global south: an in depth analysis. *Npj Climate Action* 3 (1), 47. <https://doi.org/10.1038/s44168-024-00133-1>.
- Amirkhani, M., Zarei, H., Radmanesh, F., Pande, S., 2022. An operational sociohydrological model to understand the feedbacks between community sensitivity and environmental flows for an endorheic lake basin, lake Bakhtegan, Iran. *J. Hydrol.* 605, 127375. <https://doi.org/10.1016/j.jhydrol.2021.127375>.
- Awad, D.A., Masoud, H.A., Hamad, A., 2024. Climate changes and food-borne pathogens: the impact on human health and mitigation strategy. *Clim. Change* 177 (6), 92. <https://doi.org/10.1007/s10584-024-03748-9>.
- Basegmez, H., Onalan, O., 2018. Prediction of gross domestic product (GDP) by using grey cobb-douglas production function. *Pressacademia* 7 (1), 18–23. <https://doi.org/10.17261/Pressacademia.2018.850>.
- Brown Jr., G., 1968. The California Water Project: is Public Decision making Becoming more Efficient? *Water Resour. Res.* 4 (3), 463–470. <https://doi.org/10.1029/WR004i003p00463>.
- Chen, S., Chen, B., 2016. Urban energy–water nexus: a network perspective. *Appl. Energy* 184, 905–914. <https://doi.org/10.1016/j.apenergy.2016.03.042>.
- Chen, X., Wang, D., Tian, F., Sivapalan, M., 2016. From channelization to restoration: Sociohydrologic modeling with changing community preferences in the Kissimmee River Basin, Florida. *Water Resour. Res.* 52 (2), 1227–1244. <https://doi.org/10.1002/2015WR018194>.
- Cobb, C.W., Douglas, P.H., 1928. A theory of production. *Am. Econ. Rev.* 18 (1), 139–165.
- Coletta, V.R., Pagano, A., Zimmermann, N., Davies, M., Butler, A., Fratino, U., Giordano, R., Pluchinotta, I., 2024. Socio-hydrological modelling using participatory system dynamics modelling for enhancing urban flood resilience through blue-green infrastructure. *J. Hydrol.* 636, 131248. <https://doi.org/10.1016/j.jhydrol.2024.131248>.
- Colther, C., Doussoulin, J.P., 2024. Recent applications and Developments of the Cobb–Douglas Function: from Productivity to Sustainability. *J. Knowl. Econ.* <https://doi.org/10.1007/s13132-024-02061-1>.
- Di Baldassarre, G., Viglione, A., Carr, G., Kuil, L., Salinas, J.L., Blöschl, G., 2013. Socio-hydrology: conceptualising human–flood interactions. *Hydrol. Earth Syst. Sci.* 17 (8), 3295–3303. <https://doi.org/10.5194/hess-17-3295-2013>.
- Dobbs, G.R., Liu, N., Caldwell, P.V., Miniat, C.F., Sun, G., Duan, K., Bolstad, P.V., 2023. Inter-basin surface water transfers database for public water supplies in conterminous United States, 1986–2015. *Sci. Data* 10 (1), 255. <https://doi.org/10.1038/s41597-023-02148-5>.
- Dong, J., Chen, X., Li, Y., Gao, M., Wei, L., Tangdamrongsu, N., Crow, W.T., 2023. Inter-basin water transfer effectively compensates for regional unsustainable water use. *Water Resour. Res.* 59 (12), e2023WR035129. <https://doi.org/10.1029/2023WR035129>.

- Du, E., Wu, F., Jiang, H., Guo, N., Tian, Y., Zheng, C., 2023. Development of an integrated socio-hydrological modeling framework for assessing the impacts of shelter location arrangement and human behaviors on flood evacuation processes. *Hydrol. Earth Syst. Sci.* 27 (7), 1607–1626. <https://doi.org/10.5194/hess-27-1607-2023>.
- Elshafei, Y., Sivapalan, M., Tonts, M., Hipsey, M.R., 2014. A prototype framework for models of socio-hydrology: identification of key feedback loops and parameterisation approach. *Hydrol. Earth Syst. Sci.* 18 (6), 2141–2166. <https://doi.org/10.5194/hess-18-2141-2014>.
- Faúndez, M., Alcayaga, H., Walters, J., Pizarro, A., Soto-Alvarez, M., 2023. Sustainability of water transfer projects: a systematic review. *Sci. Total Environ.* 860, 160500. <https://doi.org/10.1016/j.scitotenv.2022.160500>.
- Feng, M., Liu, P., Li, Z., Zhang, J., Liu, D., Xiong, L., 2016. Modeling the nexus across water supply, power generation and environment systems using the system dynamics approach: Hehuang Region, China. *J. Hydrol.* 543, 344–359. <https://doi.org/10.1016/j.jhydrol.2016.10.011>.
- Flörke, M., Schneider, C., McDonald, R.I., 2018. Water competition between cities and agriculture driven by climate change and urban growth. *Nat. Sustainability* 1 (1), 51–58. <https://doi.org/10.1038/s41893-017-0006-8>.
- Forrester, J. W. (1968). *Principles of Systems*. Pegasus Communications.
- Garrick, D., De Stefano, L., Yu, W., Jorgensen, I., O'Donnell, E., Turley, L., Aguilar-Barajas, I., Dai, X., de Souza Leão, R., Punjabi, B., Schreiner, B., Svensson, J., Wight, C., 2019. Rural water for thirsty cities: a systematic review of water reallocation from rural to urban regions. *Environ. Res. Lett.* 14 (4), 043003. <https://doi.org/10.1088/1748-9326/ab0db7>.
- Government of the People's Republic of China. (2023). China Issues Guideline on National Water Network Construction. Gov.Cn. https://english.www.gov.cn/policies/latestreleases/202305/26/content_WS646fe905c6d03ffcca6ed649.html.
- Griffiths-Sattenspiel, B., Wilson, W., 2009. The carbon footprint of water [Report]. River Network. <https://www.rivernetwork.org/resource/the-carbon-footprint-of-water/>.
- He, C., Liu, Z., Wu, J., Pan, X., Fang, Z., Li, J., Bryan, B.A., 2021. Future global urban water scarcity and potential solutions. *Nat. Commun.* 12 (1), 4667. <https://doi.org/10.1038/s41467-021-25026-3>.
- He, X., He, Q., Oki, T., 2025. A system dynamics model to evaluate historical and future trend of water scarcity in Beijing. *Environ. Res. Lett.* 20 (11), 114011. <https://doi.org/10.1088/1748-9326/ae0e86>.
- Hebei Provincial Bureau of Statistics. (2023). Hebei Province 2023 Statistical Bulletin on National Economic and Social Development. Hebei Provincial Bureau of Statistics. <https://www.hebei.gov.cn/columns/3bbf017c-0e27-4cac-88c0-c5cac90ecd73/202403/06/c5cd8698-2ec9-40d5-9a4b-5f4128266bd0.html>.
- Henson, P., 1994. Population growth, environmental awareness, and policy direction. *Popul. Environ.* 15 (4), 265–278. <https://doi.org/10.1007/BF02208460>.
- Housh, M., Cai, X., Ng, T.L., McIsaac, G.F., Ouyang, Y., Khanna, M., Sivapalan, M., Jain, A.K., Eckhoff, S., Gasteeyer, S., Al-Qadi, I., Bai, Y., Yaeger, M.A., Ma, S., Song, Y., 2015. System of Systems Model for Analysis of Biofuel Development. *J. Infrastruct. Syst.* 21 (3), 04014050. [https://doi.org/10.1061/\(ASCE\)IS.1943-555X.0000238](https://doi.org/10.1061/(ASCE)IS.1943-555X.0000238).
- Institute of China Geological Environment Monitoring (ICGEM). (2018). China Geological Environment Monitoring: Annual Groundwater Yearbook [in Chinese]. Vastplain House.
- Ji, jingru, Zhang, jingwen, Li, zejun, Jia, D., Ma, C., Lei, X., He, L., 2025. An evolutionary analysis of water and carbon footprints in the water receiving areas of the middle route of the South-to-North Water Transfer Project. *South-to-North Water Transf. Water* 1–15.
- Jia, B., Zhou, J., Zhang, Y., Tian, M., He, Z., Ding, X., 2021. System dynamics model for the coevolution of coupled water supply-power generation-environment systems: Upper Yangtze river Basin, China. *J. Hydrol.* 593, 125892. <https://doi.org/10.1016/j.jhydrol.2020.125892>.
- Kumar, V., & Lal, S. (2017). Stability analysis of logistic growth model with immigration effect. Unpublished. Doi: 10.13140/RG.2.2.26575.46245.
- Larsen, T.A., Hoffmann, S., Lüthi, C., Truffer, B., Maurer, M., 2016. Emerging solutions to the water challenges of an urbanizing world. *Science* 352 (6288), 928–933. <https://doi.org/10.1126/science.aad8641>.
- Li, J., Wai, O.W.H., Li, Y.S., Zhan, J., Ho, Y.A., Li, J., Lam, E., 2010. Effect of green roof on ambient CO₂ concentration. *Build. Environ.* 45 (12), 2644–2651. <https://doi.org/10.1016/j.buildenv.2010.05.025>.
- Liu, Y., Xin, Z., Sun, S., Zhang, C., Fu, G., 2023. Assessing environmental, economic, and social impacts of inter-basin water transfer in China. *J. Hydrol.* 625, 130008. <https://doi.org/10.1016/j.jhydrol.2023.130008>.
- Long, Y., Liu, Y., Zhao, T., Zhang, Z., Lei, X., Yang, Y., 2024. Optimal allocation of water resources in the middle route of south-to-north water diversion project based on multi-regional input-output model. *J. Hydrol.* 637, 131381. <https://doi.org/10.1016/j.jhydrol.2024.131381>.
- Mardani, A., Streimikiene, D., Cavallaro, F., Loganathan, N., Khoshnoudi, M., 2019. Carbon dioxide (CO₂) emissions and economic growth: a systematic review of two decades of research from 1995 to 2017. *Sci. Total Environ.* 649, 31–49. <https://doi.org/10.1016/j.scitotenv.2018.08.229>.
- Morris, J., Sokolov, A., Reilly, J., Libardoni, A., Forest, C., Paltsev, S., Schlosser, C.A., Prinn, R., Jacoby, H., 2025. Quantifying both socioeconomic and climate uncertainty in coupled human–earth systems analysis. *Nat. Commun.* 16 (1), 2703. <https://doi.org/10.1038/s41467-025-57897-1>.
- Ng, T.L., Eheart, J.W., Cai, X., Braden, J.B., 2011. An agent-based model of farmer decision-making and water quality impacts at the watershed scale under markets for carbon allowances and a second-generation biofuel crop. *Water Resour. Res.* 47 (9), 2011WR010399. <https://doi.org/10.1029/2011WR010399>.
- Niu, X., 2022. The first stage of the middle-line South-to-North water-transfer project. *Engineering* 16, 21–28. <https://doi.org/10.1016/j.eng.2022.07.001>.
- Pannocchia, G., Brambilla, A., 2007. How auxiliary variables and plant data collection affect closed-loop performance of inferential control. *J. Process Control* 17 (8), 653–663. <https://doi.org/10.1016/j.jprocont.2007.01.010>.
- Ramanathan, V., Xu, Y., Versaci, A., 2021. Modelling human–natural systems interactions with implications for twenty-first-century warming. *Nat. Sustainability* 5 (3), 263–271. <https://doi.org/10.1038/s41893-021-00826-z>.
- Richardson, G. P. (2020). Core of System Dynamics. In *System Dynamics—Theory and Application* (Second). Springer.
- Siddik, M.A.B., Dickson, K.E., Rising, J., Ruddell, B.L., Marston, L.T., 2023. Interbasin water transfers in the United States and Canada. *Sci. Data* 10 (1), 27. <https://doi.org/10.1038/s41597-023-01935-4>.
- Sobol', I.M., 2001. Global sensitivity indices for nonlinear mathematical models and their Monte Carlo estimates. *Math. Comput. Simul.* 55 (1–3), 271–280. [https://doi.org/10.1016/S0378-4758\(00\)00270-6](https://doi.org/10.1016/S0378-4758(00)00270-6).
- Sun, Z., Zheng, Y., Li, X., Tian, Y., Han, F., Zhong, Y., Liu, J., Zheng, C., 2018. The Nexus of water, ecosystems, and agriculture in endorheic river basins: a system analysis based on integrated ecohydrological modeling. *Water Resour. Res.* 54 (10), 7534–7556. <https://doi.org/10.1029/2018WR023364>.
- Tan, Y., Dong, Z., Guzman, S.M., Wang, X., Yan, W., 2021. Identifying the dynamic evolution and feedback process of water resources nexus system considering socioeconomic development, ecological protection, and food security: a practical tool for sustainable water use. *Hydrol. Earth Syst. Sci.* 25 (12), 6495–6522. <https://doi.org/10.5194/hess-25-6495-2021>.
- Tsoularis, A., Wallace, J., 2002. Analysis of logistic growth models. *Math. Biosci.* 179 (1), 21–55. [https://doi.org/10.1016/S0025-5564\(02\)00096-2](https://doi.org/10.1016/S0025-5564(02)00096-2).
- United Nations (UN). (2015). Transforming Our World: The 2030 Agenda for Sustainable Development. https://www.un.org/ga/search/view_doc.asp?symbol=A/RES/70/1.
- Van Emmerik, T.H.M., Li, Z., Sivapalan, M., Pande, S., Kandasamy, J., Savenije, H.H.G., Chanana, A., Vigneswaran, S., 2014. Socio-hydrologic modeling to understand and mediate the competition for water between agriculture development and environmental health: Murrumbidgee River basin, Australia. *Hydrol. Earth Syst. Sci.* 18 (10), 4239–4259. <https://doi.org/10.5194/hess-18-4239-2014>.
- Viglione, A., Di Baldassarre, G., Brandimarte, L., Kuil, L., Carr, G., Salinas, J.L., Scoblogi, A., Blöschl, G., 2014. Insights from socio-hydrology modelling on dealing with flood risk – roles of collective memory, risk-taking attitude and trust. *J. Hydrol.* 518, 71–82. <https://doi.org/10.1016/j.jhydrol.2014.01.018>.
- Wang, H., Zhang, J., Zeng, W., 2018. Intelligent simulation of aquatic environment economic policy coupled ABM and SD models. *Sci. Total Environ.* 618, 1160–1172. <https://doi.org/10.1016/j.scitotenv.2017.09.184>.
- Wang, J., Liu, D., Guo, S., Xiong, L., Liu, P., Chen, H., Chen, J., Yin, J., Zhang, Y., 2025. Impacts of inter-basin water diversion projects on the feedback loops of water supply-hydropower generation-environment conservation nexus. *Hydrol. Earth Syst. Sci. Discuss.* 2025, 1–31. <https://doi.org/10.5194/hess-2024-399>.
- Wang, L., He, F., Zhao, Y., Wang, J., Lu, P., Ou, Z., Jia, Y., 2023. Complex network-based analysis of inter-basin water transfer networks. *Ecol. Ind.* 156, 111197. <https://doi.org/10.1016/j.ecolind.2023.111197>.
- Wigley, T.M.L., Jones, P.D., 1981. Detecting CO₂-induced climatic change. *Nature* 292 (5820), 205–208. <https://doi.org/10.1038/292205a0>.
- Wu, J., Gao, X.-J., 2013. A gridded daily observation dataset over China region and comparison with the other datasets. *Acta Geophys. Sin.* 56 (4), 1102–1111. <https://doi.org/10.6038/cig20130406>.
- Xu, J.J., Zhang, X.Q., Zhou, T., Li, Q.Q., Wang, Y.Q., 2023. Analysis of Adjustable Water volume in the Middle Route of the South-to-North Water Diversion Project after the Implementation of the Yangtze River to Han River Water Diversion Project (in Chinese). *South-to-North Water Transf. Water Sci. Technol.* 21 (04), 790–799. <https://doi.org/10.13476/j.cnki.nsbdqk.2023.0077>.
- Yu, Z., Dai, H., Yang, J., Zhu, Y., Yuan, S., 2024. Global sensitivity analysis with deep learning-based surrogate models for unraveling key parameters and processes governing redox zonation in riparian zone. *J. Hydrol.* 638, 131442. <https://doi.org/10.1016/j.jhydrol.2024.131442>.
- Zabel, F., Delzeit, R., Schneider, J.M., Seppelt, R., Mauser, W., Václavík, T., 2019. Global impacts of future cropland expansion and intensification on agricultural markets and biodiversity. *Nat. Commun.* 10 (1), 2844. <https://doi.org/10.1038/s41467-019-10775-z>.
- Zeng, Y., Liu, D., Guo, S., Xiong, L., Liu, P., Yin, J., Wu, Z., 2022. A system dynamic model to quantify the impacts of water resources allocation on water-energy-food-society (WEFS) nexus. *Hydrol. Earth Syst. Sci.* 26 (15), 3965–3988. <https://doi.org/10.5194/hess-26-3965-2022>.
- Zhang, G., Li, F., Feng, R., Wang, J., Chu, Y., Mo, X., 2025. System stability based on logistic growth model. *Procedia Comput. Sci.* 262, 795–803. <https://doi.org/10.1016/j.procs.2025.05.112>.
- Zhang, G., Su, X., Singh, V.P., Ayantobo, O.O., 2021. Appraising standardized moisture anomaly index (SIZI) in drought projection across China under CMIP6 forcing scenarios. *J. Hydrol.: Reg. Stud.* 37, 100898. <https://doi.org/10.1016/j.ejrh.2021.100898>.
- Zhao, Y., Zhang, X., Xu, J., Smith, J.S., Xia, J., Jia, H., 2023. Water-energy-environment nexus under different urbanization patterns: a sensitivity-based framework for

- identifying key feedbacks. *J. Clean. Prod.* 408, 137243. <https://doi.org/10.1016/j.jclepro.2023.137243>.
- Zhou, X., Sheng, Z., Manevski, K., Zhao, R., Zhang, Q., Yang, Y., Han, S., Liu, J., Yang, Y., 2025. Can system dynamics explain long-term hydrological behaviors? the role of endogenous linking structure. *Hydrol. Earth Syst. Sci.* 29 (1), 159–177. <https://doi.org/10.5194/hess-29-159-2025>.
- Zhu, X., Su, X., Singh, V.P., Wu, H., Niu, J., Wu, L., Chu, J., 2025. Improving synergy of the water-agriculture-ecology system in arid areas using a novel co-optimization model. *Agric Water Manag* 312, 109408. <https://doi.org/10.1016/j.agwat.2025.109408>.